공학박사학위논문

Formation of cube-on-face texture in non-oriented electrical steel

무방향성 전기강판에서의 cube-on-face 집합조직 형성에 관한 연구

2018년 2월

서울대학교 대학원
재료공학부
권 수 빈

Formation of cube-on-face texture in non-oriented electrical steel

지도교수 황 농 문

이 논문을 공학박사학위논문으로 제출함

2017년 12월

서울대학교 대학원

재 료 공 학 부

권 수 빈

권수빈의 박사학위논문을 인준함

2017년 12월

위 원 장	한 홍 남	(인)
부 위 원 장	황 농 문	(인)
위 원	박 은 수	(인)
위 원	한 찬 희	(인)
위 원	박 창 수	(인)

Abstract

Formation of cube-on-face texture in non-oriented electrical steel

Soo-Bin Kwon

Department of Material Science and Engineering

The Graduate School

Seoul National University

Electric steel sheets using the magnetic properties of iron are divided into a grain oriented electric steel sheet and a non-oriented electric steel sheet. In the case of non-oriented electrical steel, it is generally used inside a rotating motor or generator. There is a growing interest in the efficiency of electric vehicles and generators, and there is a growing demand for the production of highly efficient, non-oriented electrical steel sheets in the future. The composition, microstructure and texture must be controlled to produce high-efficiency non-oriented electrical steel sheet. Control of composition and microstructure have

already been made much progress. But it has not yet reached the control of texture.

Cube-on-face texture is known as the ideal texture for non-oriented electrical steel. However, the cube-on-face texture is not yet available. In this study, we clarified the mechanism for formation of cube-on-face texture and found the necessary conditions for obtaining cube-on-face texture in high Si steel.

In the γ → α phase transformation, the stress was applied to the specimen to confirm the formation of cube-on-face texture. Based on these results, we succeeded in forming a large-area cube-on-face texture. In addition, the cube-on-face texture could be formed through various methods using the weight of the specimen. During the γ → α phase transformation, the nucleation sites could be controlled to form the surface nucleation, which enabled the formation of cube-on-face textures from 1% Si-steel to 2% Si-steel.

Keywords : Non-oriented electrical steel; Magnetic property; Texture control; Phase transformation; Cube-on-face texture;

Student number : 2014-31049

Contents

1. Introduction

1.1 Electrical steel

Human civilization has been constantly worried about how it uses stored energy. The wind energy was used to turn the spinning wheel by using the water stored in the position energy, and the windmill was developed to use the wind power and used to grind the grain through energy conversion. In the early days of civilization, it used a small amount of energy, but through the Industrial Revolution, mankind could get a lot of energy by using combustion, which enabled the rapid development of civilization. Since the Industrial Revolution, there has been an explosion of population, which has required more energy.

Initially, steam engines were used to obtain energy through combustion. The steam engine has played a large role in helping mankind get a large amount of energy away from the limited energy source that had previously been obtained from livestock. The ship, which used manpower and wind, was transformed into a steamboat, allowing it to cross the ocean more quickly and safely. Also, instead of a wagon, steam locomotives could send goods and people across the continent faster and more. In the

20th century, mankind began to use oil, which opened the era of engine. From the start of using the engine, mankind has been able to cross the sky and the universe.

This development of mankind has been greatly influenced by finding new energy sources and how they are stored and used. The internal combustion engine is the most widely used energy source to date, but the public thinks it will not. Some problems are highlighted because environmental problems first appeared. This is because the perception of environmental pollutants inevitably generated in the process of combustion is changing negatively. Next, because oil reserves are limited, the need for new energy sources is emerging.

In this atmosphere, research has begun on whether to replace electric furnace internal combustion engines produced using environmentally friendly energy. A variety of infrastructure is needed to use electrical energy. A facility for producing and supplying electricity such as a power plant and a transformer is required and a device for converting electrical energy supplied to the other energy source such as a motor or a light bulb is also needed. Inside these devices, materials with excellent electromagnetic properties should be used, resulting in less loss and more efficient equipment.

There are many kinds of materials with excellent electromagnetic properties. [1,2] Especially rare-earth metals have very good electromagnetic properties. [3,4] However, these materials are so rare that they can not be used publicly. [5] Therefore, there is an increasing demand for Fe, which can be widely used in public but also has excellent electromagnetic characteristics.

The iron used in high-efficiency electrical equipment is Si-steel, which is made by adding Si to increase the resistance. [6,7,8] Si is a material that increases the resistance as shown in Fig. 1.1. [9] When the resistance is high, the eddy current induced by the magnetic wave is significantly reduced. When the eddy current is reduced, the loss of energy when converted from magnetic energy to electrical energy is greatly reduced. Therefore, in a transformer or a motor, generally, a material having high resistance and good magnetic property is used. [10,11]

The steel that contains Si used for generators, motors and transformers is called electrical steel. There are two main types of electrical steel. Grain-oriented electrical steel (GO) and non-oriented electrical steel (NO). GO is generally used in transformers. In a transformer, the magnetic force changes only in one direction as shown in Fig.1.2 High-quality GO is essential

for high-efficiency transformers. [12]

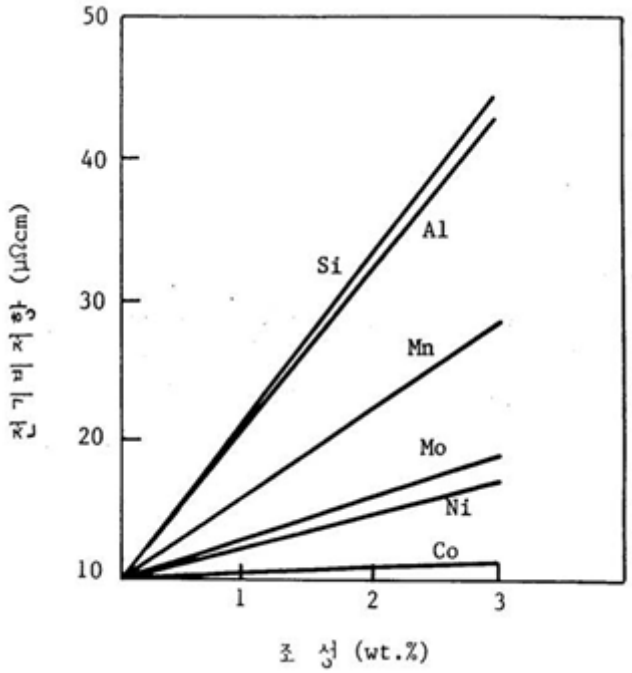

Fig 1.1 Graph of the change in electrical resistivity when each element is added to Fe.

1

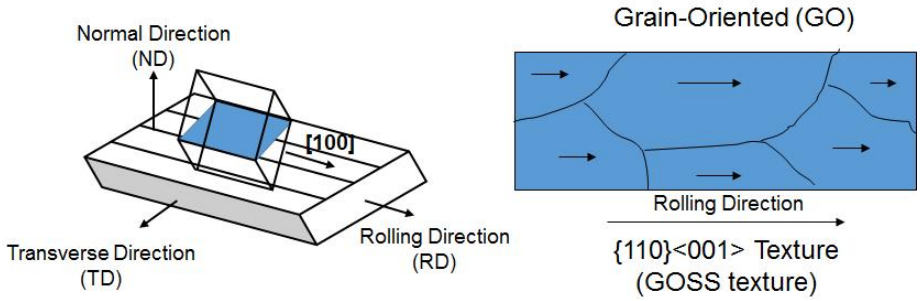

Fig 1.2 Schematics of grain-oriented electrical steel. Goss texture is commonly used for grain-oriented electrical steel.

1.2 Non-oriented electrical steel & cube-on-face texture

Over 12 million tons electrical steels are produced annually, around 80% of which are non-oriented grades. The increasing demands for efficient electrical power generation and distribution equipment are strong driving force for the development of non-oriented electrical steel with lower magnetic losses and higher permeability [13].

Demand for non-oriented electrical steel sheets is expected to increase explosively in the future. This is because various policy attempts to convert an internal combustion engine vehicle into an electric motor vehicle have been taking place recently. [14,15] As a result, there is a growing demand for high efficiency motors. In addition, the need for more electricity due to the increase in electricity demand is emerging, but the need for high efficiency generators is also increasing due to the withdrawal of large-scale nuclear power plants. [16]

In this context, optimization of composition, microstructure, composition of texture and microstructure to determine the magnetic properties of nonoriented electrical steel sheet has already achieved many results. [17,18] Texture, however, is currently not forming the ideal texture of nonoriented electrical

steel. [19]

It is well-known that the ideal texture for non-oriented electrical steel is {001}<uv0>, where each grain has two <100> directions in the plane of the sheet to give excellent magnetic performances and nearly isotropic properties [20,21,22]. The strong {100} textured columnar grains are successfully developed by manganese removal and decarburization in silicon steel plates [23]. During the vacuum annealing in γ/α dual-phase or γ-phase regions, manganese removal occurs and a thin α layer forms near the sheet surface. Driven by surface energy, the {100} texture is markedly developed in the surface layer. The {100} textured columnar grains are also obtained in low and medium silicon non-oriented electrical steels by the so-called "two-step" decarburizing annealing [24,25,26]. The aim of the first annealing is to develop a fine primary recrystallized microstructure and a thin decarburized α-layer with {100} texture on the sample surface. During the second stage, the decarburization process promotes the growth of the α-layer into the middle region of the specimen. Recently, Sung et al. [27,28] prepared the strong {100} textured columnar grains by slow cooling during γ→α transformation in pure hydrogen atmosphere and in vacuum. The mechanism responsible for preparing the favorable texture is associated with the fact that the cube faces are elastically compliant so that the texture can develop in a manner consistent

with minimization of strain energy. Besides, Xie et al. also fabricated a new-type non-oriented electrical steel with high magnetic induction by phase transformation under pure hydrogen atmosphere [29].

For low-silicon non-oriented electrical steel it is possible to apply a thermal treatment that leads to the columnar-grained microstructure with a specific type of the texture by γ→α transformation under a special atmosphere. [30] In this paper, the influence of the various atmosphere conditions on the evolution of microstructure and texture during γ→α transformation is investigated for the Fe - Si non-oriented electrical steel.

2. Effect of stress on formation of cube-on-face texture in γ → α phase transformation

2.1. Introduction

Grain oriented electrical steel is widely used as a transformer core due to its low energy loss and high magnetic flux density where the position of the transformer is fixed. However, in the case where the position of the transformer is not fixed but rotating like electrical motors and generators, non-oriented electrical steel is used. [31] Recently, electrical vehicles are becoming increasingly popular and will replace the vehicles using an internal combustion engine in near future. Therefore, there is a strong demand for the development of high efficiency electrical steel for motors and generators. [32]

It is well known that the ideal texture of silicon steel for motors and generators is a cube-on-face texture, {100}<uv0>, where each grain has two <100> directions in the plane of the sheet to give excellent magnetic properties. In an effort to develop Si steel with a cube-on-face texture, Tomida et al. [ref.] used the method of removing manganese and decarburization

from Si steel plates and successfully produced Si steel with the strong {100} textured columnar grains. [33]

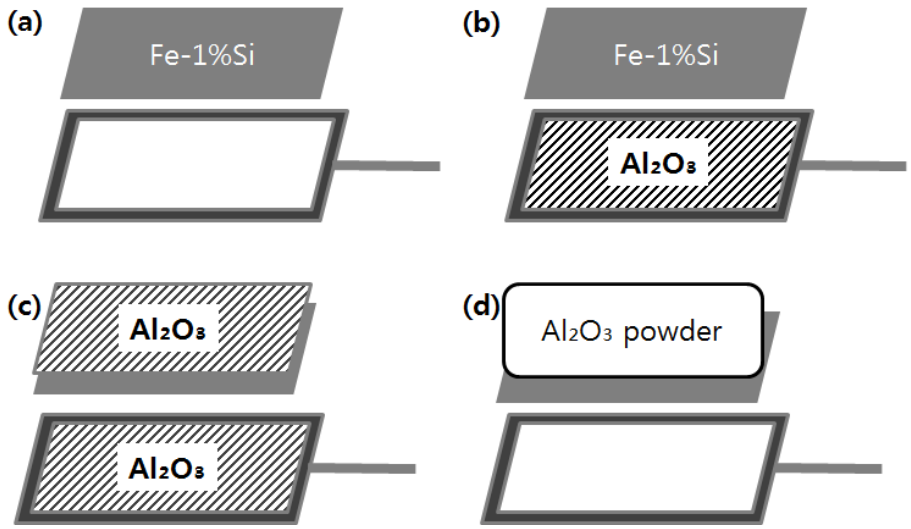

Fig. 2.1 Schematic methods of (a) non-contact, (b) 1-side contact, (c) 2-side contact and (d) contact with Al_2O_3 powder on the holder

However, this method should be done in vacuum and takes too much time in removing manganese and decarburization. To overcome such a disadvantage, Sung et al. [34] developed a new method to produce a cube-on-face texture by using the phase transformation from γ to α during cooling. However, it is not clearly understood why a cube-on-face texture is evolved during the phase transformation. This lack of understanding has been a barrier to further progress and practical applications.

When any sample is heat treated, it should be placed on some material and thereby the sample is in physical contact with the supporting material. It is normally thought that such physical contact would not affect the microstructure evolution of the sample. In the preliminary experiment of Fe-1%Si steel, however, we found out that the physical contact between the Fe-1%Si sheet sample and the Al_2O_3 plate has a strong effect on the evolution of the cube-on-face texture. The purpose of this paper is to report the effect of the physical contact on the evolution of cube-on-face texture in Fe-1%Si steel.

2.2. Experimental Details

An ingot of Fe-1wt%Si was prepared by vacuum induction melting. The ingot was hot rolled to 2.3 mm and cold rolled to

0.35 mm in thickness. The transformation temperature between α and γ was measured at the cooling and heating rate of 600℃/h with the thermogravimetric analysis (TGA)/differential scanning calorimetry (DSC) (Mettler Toledo). The measured temperatures of the Fe-1wt%Si alloy were A_{c1}=984℃, A_{c3}=1004℃, A_{r3}=975℃, and A_{r1}=952℃.

The cold-rolled sheets were heated in a tube furnace at 1 atm of flowing H_2 gas. The sheets were heated at 600℃/h to 1100℃ and annealed for 5 minutes; such a treatment would produce the γ phase. Then the sheets were cooled at 600℃/h to 950℃ during which γ is transformed to α. Then, the sheets were cooled to room temperature in the tube furnace.

To examine the effect of the physical contact on the evolution of cube-on-face texture during the phase transformation from γ to α, the rectangular rim was used as the specimen holder with the empty center as shown in Fig. 1(a), where the Fe-1%Si sheet sample would be supported by the rim but not in physical contact with the holder. The sample of Fig. 2.1 (a) is used as a reference which has no physical contact with any other solid. In Fig. 2.1 (b), the Fe-1%Si sheet sample was placed on the Al_2O_3 plate so that the top surface of the sample was exposed to the H_2 atmosphere and the bottom surface was in physical contact

with the Al_2O_3 plate. In Fig. 2.1 (c), the additional Al_2O_3 plate was placed on the sheet sample in Fig. 2.1 (b) so that both sides of the sample were in physical contact with the Al_2O_3 plate. To confirm whether the evolution of the cube-on-face texture might come from any chemical effect coming from Al_2O_3 or from the physical contact, Al_2O_3 powder was placed on the sample as shown in Fig.1(d). Further, the effect of the physical contact was also examined for tungsten and quartz plates whose results are shown in Fig. 2.4.

The surface texture of the heat-treated sheet samples was measured by analyzing the grain orientation using an electron back-scattered diffraction (EBSD) system (TSL), mounted on a field-emission scanning electron microscope (FE-SEM) (JSM-7600F). EBSD was measured on the area of 6.8 mm × 5 mm at the center of the sample surface.

2.3. Results & Discussions

Figure 2 shows the inverse pole figure (IPF) map and the orientation distribution function (ODF) at ϕ_2 =45^0-section analyzed by EBSD for samples of Fig. 1(a) and (b). Figures 2(a) and (b) shows the IPF maps respectively for the top and bottom surfaces of the sample for Fig. 1(a). They show a random

texture without any noticeable {100} orientation, which is also confirmed by Figs. 2(e) and (f), which are respectively ODFs of Figs. 2(a) and (b). The area percentage of a cube-on-face texture was determined by the orientation within {100} $\pm 15^0$. Percentages of a cube-on-face texture in Fig. 2(a) and (b) were respectively 11.6% and 14.1%. (See Table 1)

Figures 2(c) and (d) show the IPF maps respectively for the top and bottom surfaces of the sample for Fig. 1(b). The IPF map on the top surface in Fig. 2(c) shows a slightly cube-on-face texture, which is also confirmed by the ODF in Fig. 2(g). It should be reminded that the top surface was in Fig. 2(c) not in physical contact with any other solid. However, the IPF map on the bottom surface in Fig. 2(d) shows a strong cube-on-face texture, which is also confirmed by the ODF in Fig. 2(h). Figure 2(d) indicates that the physical contact with the Al_2O_3 plate has a strong effect on the evolution of the cube-on-face texture.

Percentages of a cube-on-face texture in Fig. 2(c) and (d) were respectively 36.1% and 52.8%. There is the texture difference of 16.7% between the top and bottom surfaces. It appears that the high percentage (52.8%) of a cube-on-face texture in Fig. 2(d) comes from the physical contact with the

Al2O3 Plate. Although the top surface in Fig. 2-(c) was not in physical contact, it has a much higher percentage of 36.1% than those of the top and bottom surfaces respectively in Fig. 2(a) and (b). (See Table 1). The relatively high percentage of 36.1% in Fig. 2(c) would be attributed to the fact that the grains of a cube-on-face texture were formed first on the bottom surface, which was in contact with the Al_2O_3 plate, grew to the top surface across 350 ㎛ thickness of the sheet sample.

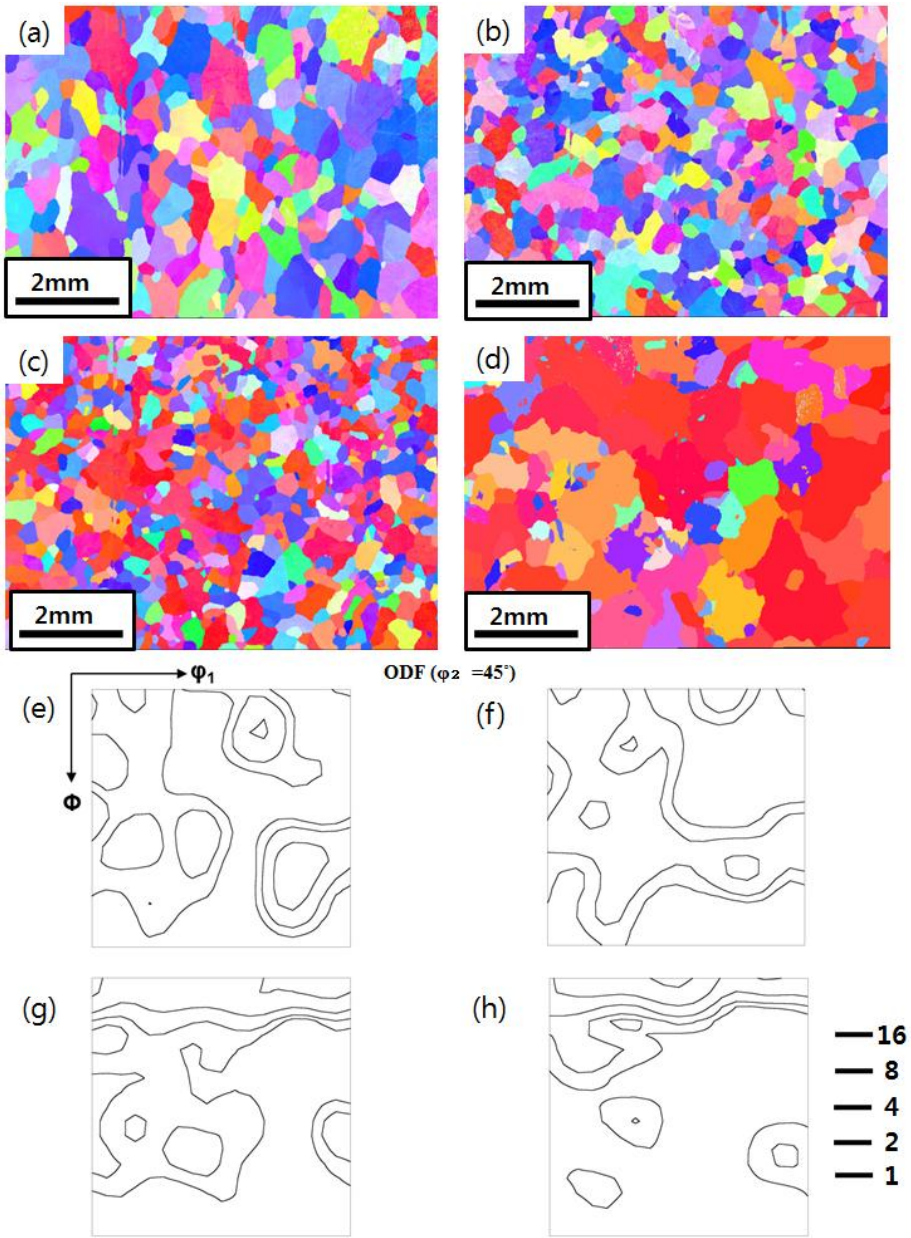

Fig. 2.2 The texture of (a) top surface of Fig. 2.1-(a), (b) bottom surface of Fig. 2.1-(a), (c) top surface of Fig. 2.1-(b), and (d) bottom surface of Fig. 2.1-(b). The ODF image (ϕ_2 =45^0) of top surface of Fig. 2.1-(a), (b) bottom surface of Fig. 2.1-(a), (c) top surface of Fig. 2.1-(b), and (d) bottom surface of Fig. 2.1-(b)

Figures 2.3(a) and (b) show the IPF maps respectively for the top and bottom surfaces of the sample for Fig. 1(c). Both show a strong cube-on-face texture, which is also confirmed by the ODFs in Figs. 2.3(e) and (f). Percentages of a cube-on-face texture in Fig. 2.3(a) and (b) were respectively 64.5% and 76.0%. Comparison of these results with those of Figs. 2(a), (b) and (c) indicates that the physical contact with the Al_2O_3plate should enhance the evolution of a cube-on-face texture.

To confirm the possibility that the physical contact with the Al_2O_3 plate should provide any source for chemical interactions with the sample surface, Al_2O_3 powder was placed on the sample surface as shown in Fig. 2.1(d). Figures3(c) and (d) show the IPF maps respectively for the top and bottom surfaces of the sample for Fig. 1(d). Both show a random texture, which is also confirmed by the ODFs in Figs. 2.3(g) and (h). Percentages of a cube-on-face texture in Fig. 2.3(c) and (d) were respectively 12.2% and 10.8%. These results indicate that the evolution of a cube-on-face texture should come from any force such as the friction from the contact rather than from any chemical interaction with Al_2O_3.

Then, the physical contact with other plates such as tungsten and quartz is expected to have a similar effect. Additional

experiments with tungsten and quartz plates were performed with the Fe-1%Si sample sheet sandwiched by the plate as shown in Fig. 2.1(c). Both samples show strong a cube-on-face texture as revealed in ODFs of Figs. 2,4(a) and (b), which are respectively for tungsten and quartz.

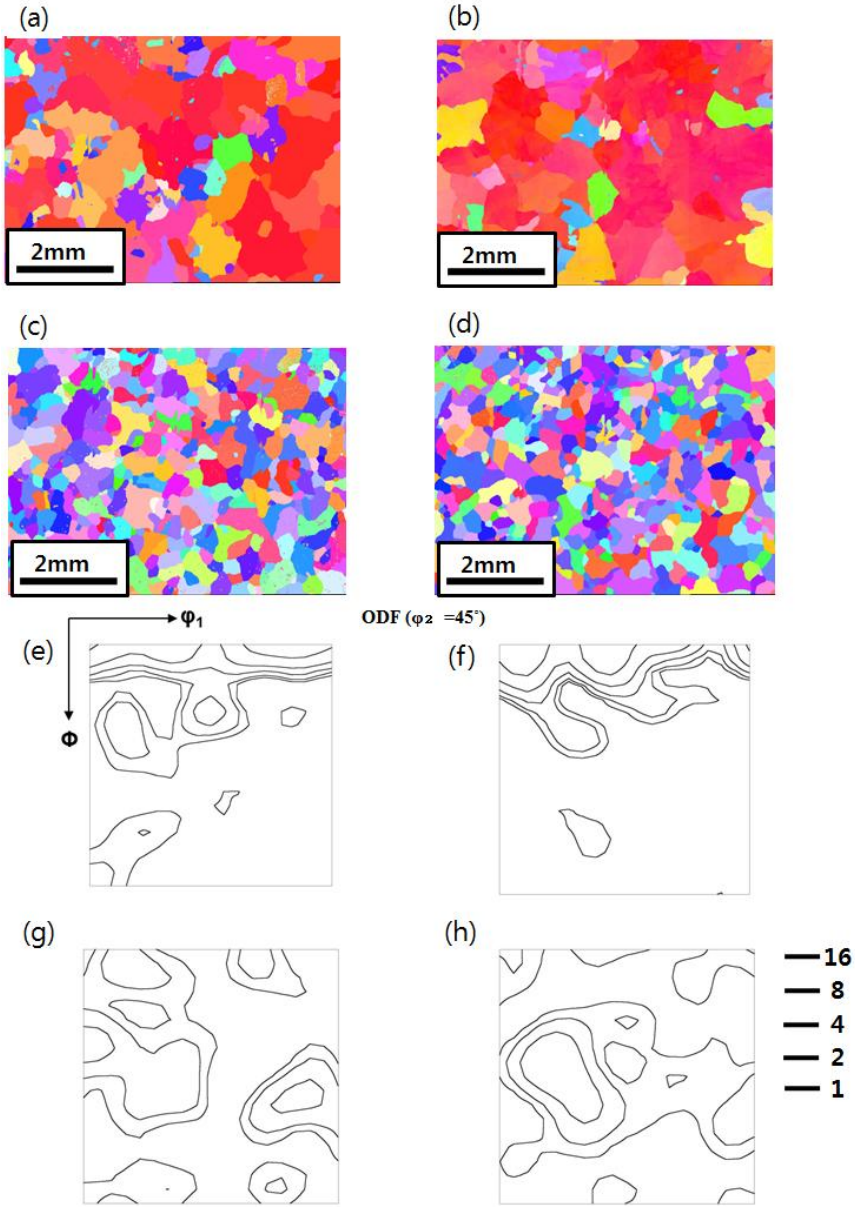

Fig 2.2 The texture of (a) top surface of Fig. 2.1-(c), (b) bottom surface of Fig. 2.1-(c), (c) top surface of Fig. 2.1-(d), and (d) bottom surface of Fig. 2.1-(d). The ODF image (ϕ_2 =45^0) of top surface of Fig. 2.1-(c), (b) bottom surface of Fig. 2.1-(c), (c) top surface of Fig. 2.1-(d), and (d) bottom surface of Fig. 2.1-(d)

Experiment #	Plane	{001}area% (±15°)	Contact surface
Fig.2.1-(a)	Top	11.6%	X
	Bottom	14.1%	X
Fig.2.1-(b)	Top	36.1%	X
	Bottom	52.8%	O
Fig.2.1-(c)	Top	64.5%	O
	Bottom	76.0%	O
Fig.2.1-(d)	Top	12.2%	X
	Bottom	10.8%	X

Table 2.1 {001} area% (±15°) and whether surface contact with Al_2O_3 plate of each surface

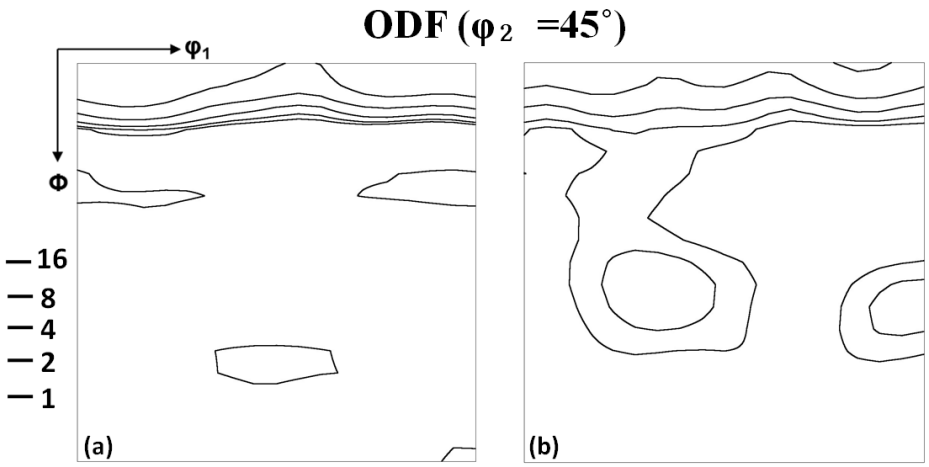

Fig 2.4 The ODF image (ϕ_2 =45°) of (a) surface contact with quartz and (b) surface contact with W

The results of Figs. 2,2, 2,3 and 2,4 indicate that the physical contact should be closely related with the evolution of a cube-on-face texture. Which effect would be possible by the physical contact? One possibility would be that the frictional force between the plate and the sample surface might affect the nucleation barrier of surface grains with normal direction (ND)//{100} in the transformation from γ to α during cooling. The thermal expansion coefficient of Fe is 12 and those of Al_2O_3, tungsten and quartz are respectively 5.5, 4.5 and 0.5 [ref.]. During cooling, the Fe-1%Si sheet would be shrinking more than Al_2O_3, tungsten and quartz plates and the friction between the sheet and plate would generate the slight tensile shear stress on the sheet surface. Materials such as barium, indium and tin which have a higher thermal expansion coefficient than Fe could not be tested as a plate because of their low melting points. Then, how would the slight tensile shear stress affect the evolution of a cube-on-face texture.

For this question, it is worth mentioning Sung et al.'s previous suggestion [ref.] for the evolution of a cube-on-face texture during γ → α transformation.

There is a volume increase when BCC α is nucleated from FCC γ and the α nucleus would be under compressive stress, which

would increase the nucleation barrier. The strain energy arising from the compress stress would be proportional to the Young's modulus of α. As a result, the strain energy should increase the nucleation barrier of α. The nucleation barrier would decrease with decreasing Young's modulus of α, which depends on the direction and is minimum for {100} directions. Therefore, when the α nucleus has the {100} directions normal to the compressive stress arising from γ → α transformation, the nucleation barrier would be minimum. Since the compressive stress on the surface is absent in the direction normal to the surface, the cube-on-face grains would have a minimum nucleation barrier. Therefore, when nucleation takes place on the surface, the cube-on-face grains would be favored. [35~38]

According to this analysis, the cube-on-face texture is expected to evolve when nucleation takes place dominantly on the surface. However, the results of Figs. 2.2(a) and (b), where the sheet sample has no physical contact, shows that the cube-on-face texture was not evolved. [39] The results of Figs. 2.2(a) and (b) appear to disagree with Sung's suggestion [ref.] In order that Sung's suggestion may agree with Figs. 2.2(a) and (b), nucleation should not take place exclusively on the surface but take place appreciably inside the bulk. This means that the nucleation barrier inside the bulk should be lower than that on

the surface. For example, the nucleation site of quadruple points inside the bulk can be lower than that of triple junction on the surface. [40]

On the other hand, the results of Figs. 2.3(a) and (b) as well as Figs. 2.4 show that when the sheet sample has physical contact, the cube-on-face texture was evolved. These results can be explained if it is assumed that the slight tensile shear stress from physical contact decreases the compressive stress on the surface and thereby lowers the nucleation barrier on the surface than that inside the bulk.

3. Process of cube-on-face texture large sheet using tile

3.1 Effect of big size tile on formation of cube-on-face texture in large size sheet

The samples used in the previous chapter are all 15mm x 35mm. The size of the specimen to be loaded on the holder is 15mm X 35mm, so the experiment was conducted with a relatively small specimen. However, in order to mass-produce, we need larger size specimens than the sample above. In order to measure the magnetic properties, a test specimen of at least 50 mm x 50 mm is required, which necessitates the experiment of large size sheets.

In the previous chapter, we succeeded in forming a cube-on-face texture using one Al2O3 plate on one side. The experiment was carried out using a single Al2O3 plate in a 50 mm × 50 mm specimen. (Fig. 3.1). In the heat treatment conditions, the experiment was carried out to check whether the cube-on-face texture was formed in a shorter time by loading and unloading the specimen unlike the previous experiment.

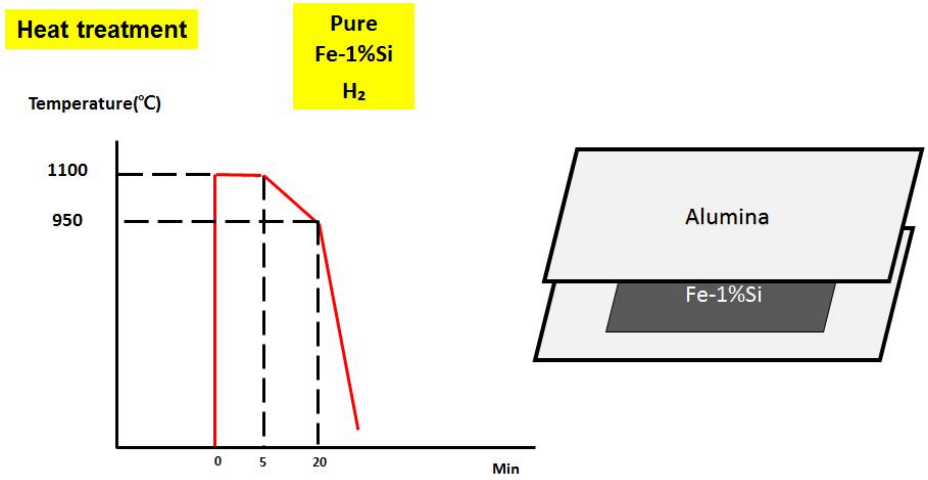

Fig. 3.1 Schematic image of heat treatment and experiment condition.

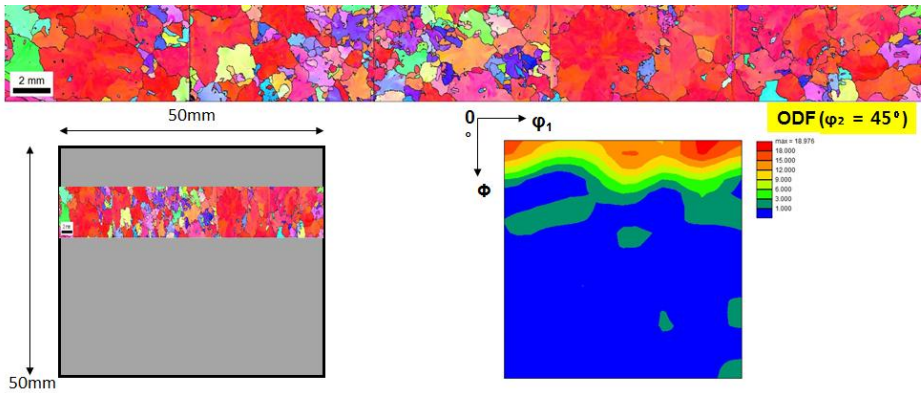

Fig 3.2 Texture of 10㎜ X 50㎜ region on 50㎜ X 50㎜ sized specimen. The ODF image (ϕ_2 =45^0) of the same region.

Unlike the previous 50mm x 50mm specimens, it was thought that measuring narrow areas with EBSD was insufficient to investigate the overall texture formation. Therefore, the specimen was finely divided into 10mm x 10mm as shown in Fig. 6, and 5 samples were subjected to the whole area EBSD analysis. The results were combined and a large area of 10 mm X 50 mm could be analyzed by EBSD.

Analysis of the specimens by EBSD showed that the cube-on-face texture was formed in a large part of the specimen. This was predicted by the effects of physical contact found in the previous chapter. It was confirmed that a very high fraction (001) texture was formed by IPF and ODF. In the middle of the sample, however, there was a part where there was no cube-on-face texture at all. If this phenomenon continues to occur in a large-area process, it will have a negative impact on the magnetic properties. Therefore, there is a need for research to reduce this area.

The IPF image in Fig. 3.2 shows that random texture is formed in the middle part. Considering the results of Chapter 2, we can conclude the following conclusions. If the physical contact with

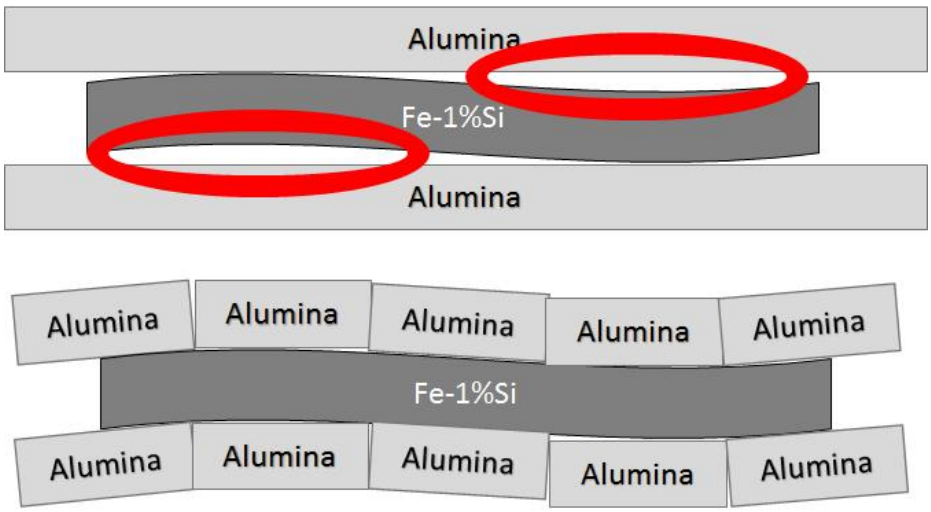

Fig 3.3 Schematic image of difference between one large plate and several small plates

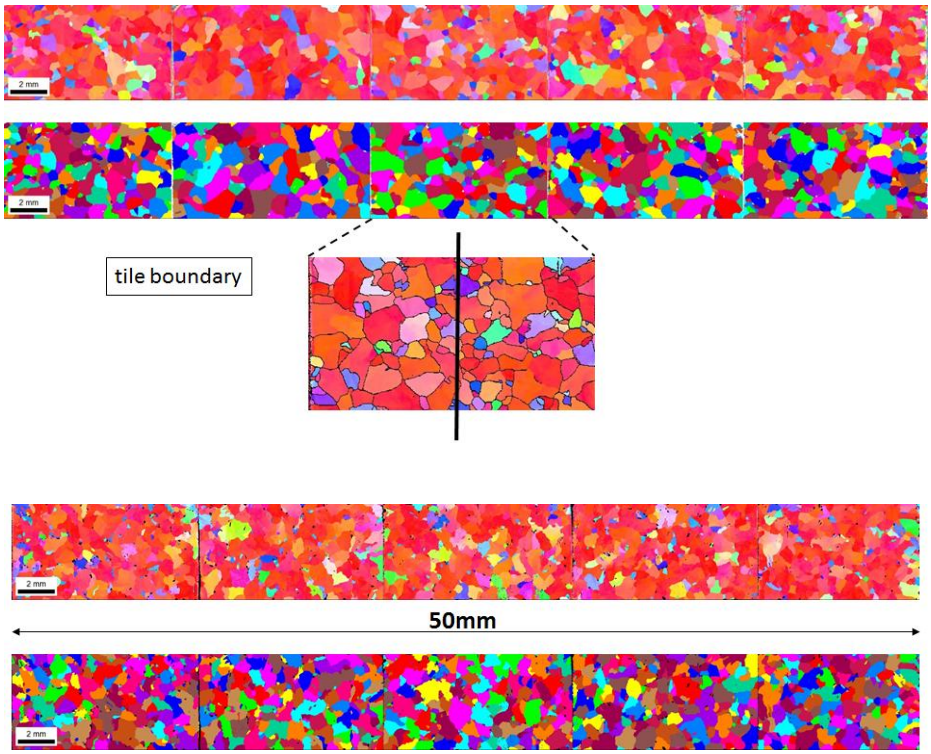

Fig 3.4 2 Texture of 10㎜ X 50㎜ region on 50㎜ X 50㎜ sized specimen. Upper IPF image of specimen made by 30㎜ X 30㎜ sized Al_2O_3 plates. Lower IPF image of specimen made by 10㎜ X 10㎜ sized Al_2O_3 plate

the Al2O3 plate plays a very important role in the formation of the cube-on-face texture, it can be concluded that the portion where the random texture is formed has not been contacted.

Fig. 3.3, the area marked with a red circle is a part that is inevitably inaccessible because the Al2O3 plate is a large plate. In this part, it was thought that the cube-on-face texture would not be formed as shown above.

3.2 Effect of a number of small size tiles on formation of cube-on-face texture in large size sheet

In order to solve this problem, several small tiles were used as shown in Fig. If you use a small tile, you will be able to minimize the non-contact portion of the sample and the plate and then form a cube-on-face texture with a higher area fraction.

Based on the above idea, the following experiment was conducted. All conditions were the same, but experiments were carried out to reduce the untouched parts of Al2O3 plates contacting the sample with several 30mm x 30mm and 10mm x 10mm, respectively. The results are shown in Fig. 8. As can be seen from the IPF image, the smaller the tile size, the better the cube-on-face texture is in all areas. The nucleation due to

contact is generally well formed on the specimen, and all (001) is formed in the phase-change section.

Through this experiment, it was once again confirmed that contact with the plate is an essential component of the cube-on-face texture. We also found that large-area specimens can form cube-on-face textures. Based on these facts, we were able to go one step closer to mass production.

4. Effect of uniaxial stress on cube-on-face texture formation

4.1 Introduction

The results of Chapter 2 and 3 support the fact that 2D-stress is applied to the surface due to the difference in thermal expansion coefficient due to contact, which is very important for the formation of the cube-on-face texture in the phase transition. To summarize, surface nucleation and 2D stress are essential to obtain the ideal texture of non-oriented electrical steel, cube-on-face. Surface nucleation can be induced by various methods, but it is not easy to apply 2D stress during annealing. It is difficult to stress considerably because stress must be applied uniformly in various directions.[41~42]

In order to solve this difficult problem, the idea of using uniaxial stress which is relatively easy to apply stress was given. The idea was that if a very small uniaxial stress could be applied to the cube-on-face due to the very small stress caused by thermal expansion and friction, a similar effect would be obtained. We conducted the heat treatment at high temperature and devised an experiment to apply uniaxial stress by using

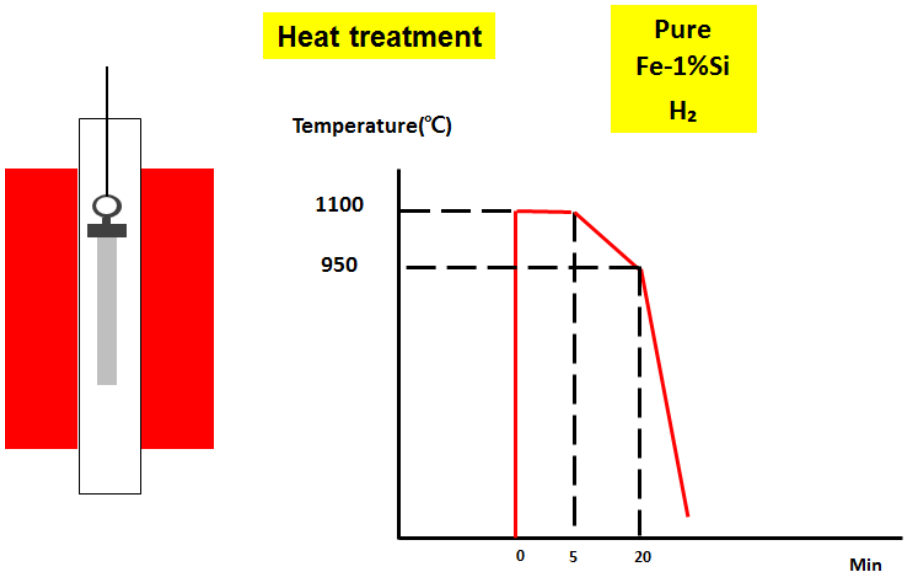

Fig 4.1 Schematic image of heat treatment and how to put self-weight on specimen during the heat treatment

gravity as its own weight in the thought that the stress due to the difference of thermal expansion would not be great. [43]

4.2 Formation of cube-on-face texture by self-weight hanging

There are several ways to apply uniaxial stress. However, it is not very common to apply uniaxial stress in high temperature heat treatment under hydrogen atmosphere. Therefore, the following experiment was conducted through considerable difficulties. [44,45] The conditions of the experiment are shown in Fig 4.1. A vertical furnace was fabricated, and the specimen was cut into a length of 30 cm and heat treated with medallion. When the heat treatment is performed in this manner, the specimen undergoes gravity stress due to its own weight during the heat treatment period. This stress, unlike previous experiments, will act in uniaxial direction, so it will be an experiment to confirm how uniaxial stress affects the formation of cube-on-face texture. The specimens were loaded at 1100°C as shown in Fig. 4.1. Held at a temperature of 1100°C for 5 minutes, and then converted to γ phase, and then cooled to 950 for 15 minutes.

The results of the experiment are shown in Fig. 10 as IPF

image. The results show that the cube-on-face texture is very well formed by uniaxial stress at the bottom of the specimen. Compared with the experimental results in Chapter 2, we can see that the results are different from those of the reference without contact. Despite the fact that both experiments are non-contact experiments, different textures are produced in uniaxial stressed specimens. This indicates that uniaxial stress affects the texture formation during the phase transformation process. It can be concluded that cube-on-face texture is formed by uniaxial stress as well as 2D-stress due to contact with the plate.

There is an interesting part in Fig 4.2. At the top of the hanging specimen, the area fraction of the cube-on-face texture is significantly reduced. The area fraction is shown in Fig. This shows that the area fraction at the bottom of the specimen is 40.1%, but the fraction gradually decreases to 36.5%, 21.9%, and 7.8% at the top of the specimen. These results can be confirmed in Fig. 4.2. It can be seen that the area of red cube-on-face texture gradually disappears from the upper part, and purple γ fiber is produced instead.

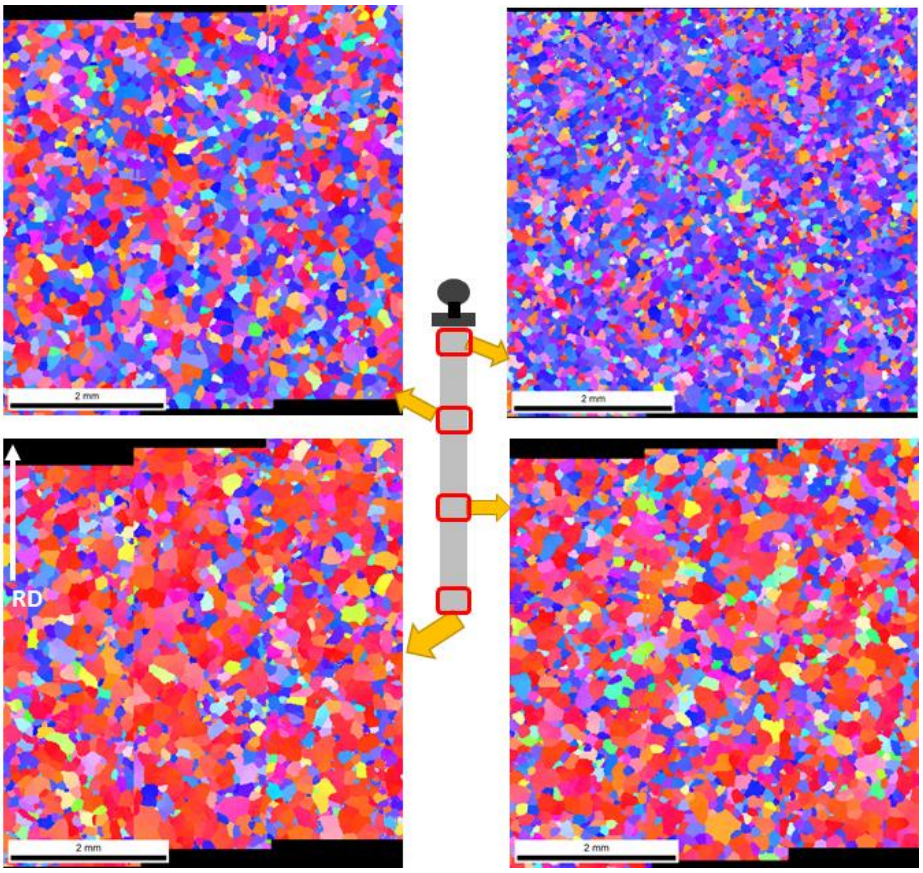

Fig 4.2 The texture at each location of self-weight experiment

These results lead to the following conclusions. If the applied stress exceeds a certain value, the cube-on-face texture is not formed. That is, when a specific stress is applied, a cube-on-face texture is formed in the phase transformation process, and the stress that satisfies this condition can be interpreted as being very small. Thus, when very small uniaxial stresses are applied, it can be concluded that a cube-on-face texture is formed.

The stress acting on each part is calculated and shown in Fig. 4.3. The stress acting on the specimen is very small. Units are expressed in Pa, not Mpa, which is negligible in general mechanical properties measurements. However, when compared with the results in Fig. 4.2, it can be seen that this small uniaxial stress has a great influence on the texture formation in the phase transform process. In other words, very small uniaxial stresses control texture formation during phase transformation and small uniaxial stress of less than 100Mpa is required to form cube-on-face texture.

샘플 #	stress (Pa)	Grain size (㎛)	(001) 분율 (%)
4번	228.50	78.47	7.8
3번	153.72	108.82	21.9
2번	78.94	108.17	36.5
1번	4.08	109.81	40.1

Fig 4.3 The stress, grain size and {001} area at each location of self-weight experiment

4.3 Formation of cube-on-face texture by U-type holder

The following conclusions were obtained through previous experiments. The uniaxial stress in the phase transformation process can lead to the formation of a specific texture, and a very small amount of stress is required to form the cube-on-face texture. [46,47] It is difficult to heat treat weakly stress uniaxially. In order to generate a phase transform, a high temperature of 1100 ° C is required. At such a high temperature, the sample is easily deformed and the Young's modulus is lowered.

The self-weight hanging test at chapter 4.2 was able to apply tensile only. However, given the discussion in chapter 2, compression should have the same effect. In the γ phase, when the α phase is nucleated, it is basically subjected to compression stress, so compression should be added to improve the effect. In the case of the self-weight hanging test, it is easy to conduct experiments in a laboratory that conducts academic research, but it is very difficult to apply such a process in a company aiming at mass production. The need for new processes has arisen for a number of complex reasons.

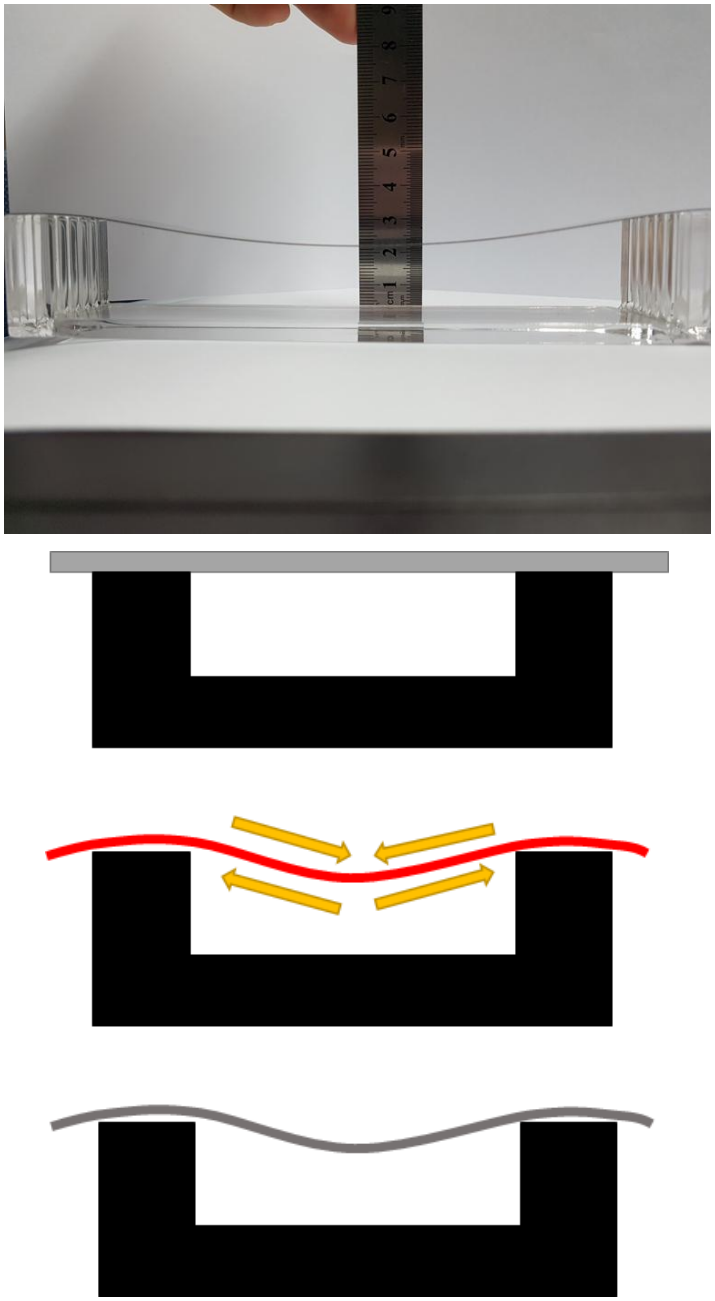

Fig 4.4 Schematic image of how to put self-weight on the U-type holder during the heat treatment.

As a result, we have devised a U-type holder of Fig. 4.4. The holder is made of quartz, 17cm long and 3cm high. The reasons for making Quartz are as follows. First, even if it receives high heat at high temperature, it reacts with Si-steel and does not stick. This allows the specimen to be easily removed from the holder after the heat treatment. Also, due to its low coefficient of thermal expansion, it does not affect the sample at high temperatures. And it can be used stably even at high temperature. For this reason, a holder was fabricated using quartz. Place the specimen on the U-type holder and proceed with the heat treatment as shown in Fig. 4.4.

Prior to the heat treatment, the specimen is laid flat on the U-type holder. However, when the temperature rises to a high temperature during the heat treatment, the specimen comes down in the middle due to its own weight. At this time, compression will be applied to the upper part of the specimen, and tension will be applied to the lower part of the specimen. In this state, the specimen will undergo a phase transformation by cooling under compression and tension. Experiments were conducted to form a cube-on-face texture in the phase transform process using these two stresses. When the heat treatment process is completed, it is confirmed that the specimen is bent downward by its own weight as shown in the image at the upper part of

Fig. 4.4. This shows that the concept of the experiment proceeded as expected.

The heat treatment cycle is shown in Fig. 4.5. Unlike the previous self-weight hang test, the specimen was placed in a U-type holder and tested under 100% hydrogen atmosphere. The specimen and holder were placed in a tube furnace to maintain the hydrogen atmosphere and N60 high purity hydrogen was used. Unlike the self-weight hang test, the specimens were heated in a furnace, not at high temperature. After heating to 1100 ° C for 115 minutes, it was maintained at 1100 ℃ for 5 minutes so that it could be transformed sufficiently into the γ phase. Thereafter, cooling was performed to 950 ℃ for 60 minutes to cause a phase transform for a sufficiently slow time. Then, the specimen was taken out from the furnace and analyzed after it had cooled sufficiently in the furnace. To investigate the effects of compression and tension on the specimens, the specimens were sampled and polished by EBSD. Fig. 4.6 shows the result of IPF and ODF, where the specimens were taken, area fraction and grain size.

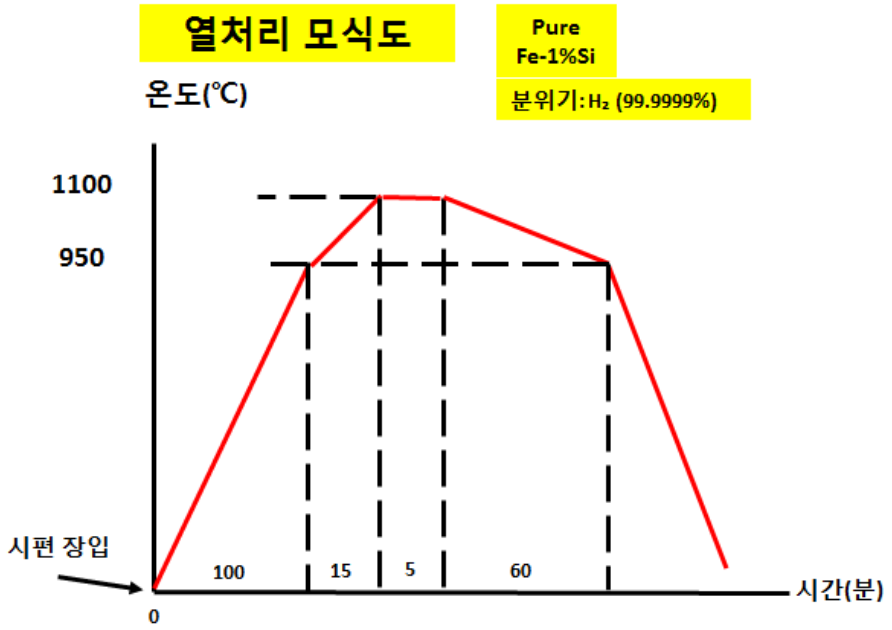

Fig 4.5 Schematic image of heat treatment on U-type holder experiment

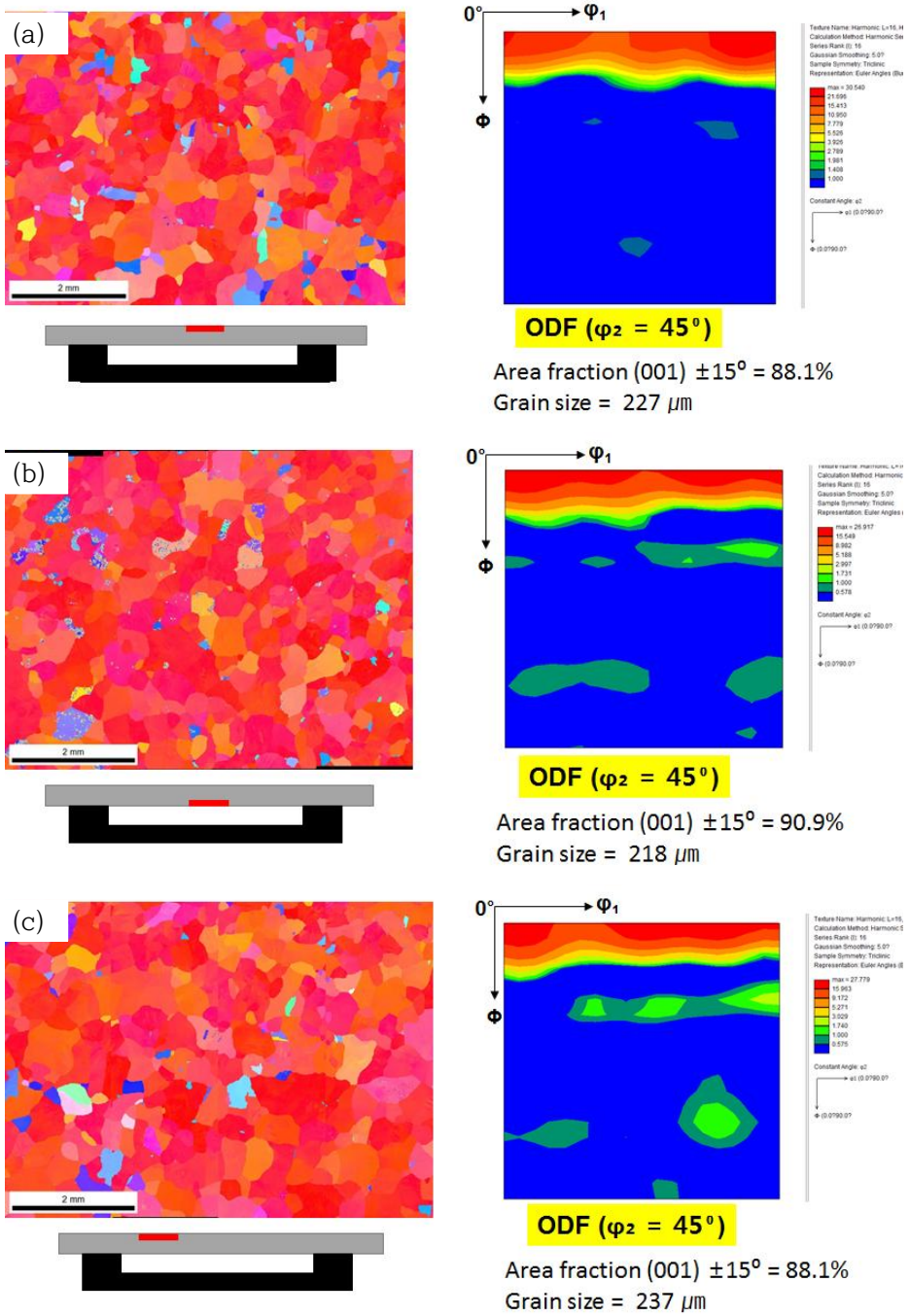

Fig 4.6 Each Texture and ODF (ϕ_2 =45°) image at other parts.

Fig 4.6-(a) is the upper part of the center of the specimen. As can be seen in Fig. 4.4, this is where compression takes place. In this area, we obtained an area fraction of very high cube-on-face texture of 88.1%. On the IPF image, we can see that the red part of the cube-on-face texture is very well developed and that the cube-on-face texture is well formed on the ODF.

Fig. 4.6-(b) is the lower part of the center of the specimen. Unlike Fig. 4.6- (a), it is the location where tensile is applied. In this part, we obtained an area fraction of very high cube-on-face texture of 90.9%. On the IPF image, we can see that the red part of the cube-on-face texture is very well developed and that the cube-on-face texture is well formed on the ODF.

Fig. 4.6-(c) is the middle part of the specimen. Unlike Fig. 4.6-(a) and (b), it is the position where tension is applied due to the weight of the center part. In this area, we obtained an area fraction of very high cube-on-face texture of 88.1%. On the IPF image, we can see that the red part of the cube-on-face texture is very well developed and that the cube-on-face texture is well formed on the ODF.

Analyzing the above data, we can first confirm that we have a very high cube-on-face area fraction in common. This shows

that the U-type holder process is much more efficient than the previous self-weight hang process. It is also shown that the cube-on-face texture is uniformly formed over a large portion of the specimen, and that this process is likely to be used on actual factory scale. [48]

The higher cube-on-face texture area fraction at the top and bottom of the center portion of the sample shows that the process using the U-type holder is efficient, as mentioned above. [49] On the other hand, the purpose of confirming the difference in cube-on-face texture formation due to compression and tension has not been reached. The difference between the upper and lower surfaces is presumably due to the fact that the thickness of the sample is as thin as 350 ㎛. The grain size of the cube-on-face texture is about 200 ㎛, regardless of its location. With this grain size, most grains grow through the normal direction. This suggests that there is no difference in the area fraction between the top and bottom surfaces.

5. Cube-on-face texture steel production with high Si content and impurities

5.1 Introduction

Summarizing the results of the previous chapters, we found that it is possible to form a cube-on-face texture with a 90% area fraction through a relatively simple process. Since cube-on-face texture is an ideal texture in NO, this process has shown the possibility of obtaining high quality NO. [50,51]

However, there are other limitations to the results of previous chapters. First, specimens with impurities suppressed were used. Fig. 5.1 shows that elements other than Fe and Si are suppressed to the maximum extent. [52] Unexpected impurities are present in a certain amount for large-scale production. There will be a clear difference between phase transforms in pure samples and those with impurities. For large-scale production, cube-on-face texture should be formed even if impurities are included to some extent. Therefore, it is necessary to confirm whether a cube-on-face texture is formed even in a composition containing an impurity. [53]

Also, the samples used in previous chapters contain 1% of Si.

As stated in the introduction to Chapter 1, high-quality electrical steel should have high Si content. [54] The highest quality NO currently produced contains 2 to 3% Si. Therefore, it is impossible to make high-quality NO by the composition of the sample used in the previous chapters. It is essential to form a cube-on-face texture in a composition containing 2% or more of Si.

I have conducted experiments to form cube-on-face textures from impurities in general, and furthermore have conducted experiments to form cube-on-face textures with compositions containing 1.5% and 2% Si.

	C	Si	Mn	P	S	Al	Ti	N	
Pure 1%Si	0.0009	0.93	<0.0005	0.001	0.0006	0.0006	<0.0005	<0.0005	
1%Si	0.0024	1	0.054	0.005	0.003	0.002	0.0016	0.0011	

Fig 5.1 Chemical composition of specimen steels

5.2 Formation of cube-on-face texture with impurities

To investigate whether impurities affect the formation of cube-on-face texture, the 1% Si composition of Fig. 5.1 was prepared. Included impurities generally contain amounts of impurities normally contained in the mass produced steel. The sample was cold rolled to a thickness of 350 ㎛. As shown in Fig. 5.2, the alumina plate was brought into contact with both surfaces in order to confirm the formation of cube-on-face texture through contact with the alumina plate. The heat treatment process is depicted on the left side of Fig. 5.2. The heat treatment temperature and time were compared under the same conditions to compare with Chapter 2. The sample was placed between the alumina plates and heated to 1100 °C in a tube furnace. And then maintained at 1100 °C for 5 minutes to allow sufficient transformation into the γ phase. In addition, cooling to 950 °C was carried out at a cooling rate of 10 °C per minute in order to induce phase transformation into α phase.

After the experiment, the specimen were sampled and polished, and the texture was analyzed by EBSD. The results were compared with those of the sample without impurities in chapter 2.

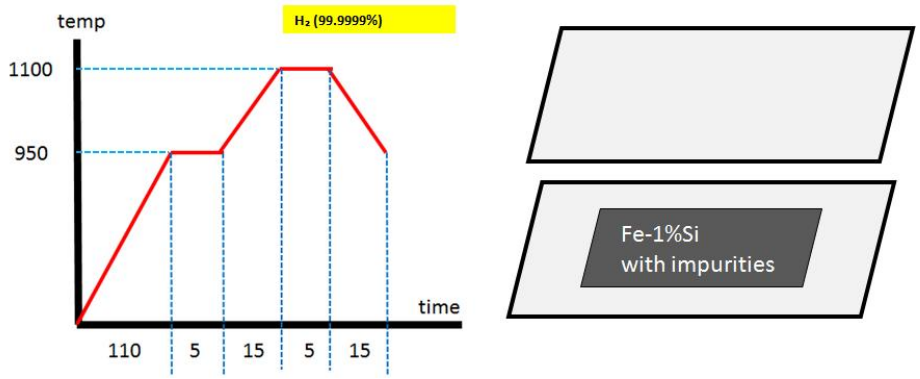

Fig 5.2 Schematic image of heat treatment on Fe-1%Si with impurities contacting Al_2O_3

IPF, ODF and data obtained by EBSD analysis are summarized in Fig. 5.3. For convenient comparison, we placed the data of the specimen containing impurities on the left side and the data of the specimen without impurities obtained in Chapter 2 on the right side.

It was confirmed that cube-on-face texture was formed during phase transformation through contact with alumina plate even in impurity-containing composition. From the left IPF image, it can be seen that the red part is widely distributed. ODF also has a well-formed cube-on-face texture line. When the data of the specimen containing the impurities are observed, it can be confirmed that the contact of the alumina plate is effective.

However, comparing the data on the left with the specimens containing no impurities shows a considerable difference. First, the area fraction of the cube-on-face texture is 76.0% when impurities are not present, but it is reduced to about 38.2% when impurities are contained. In addition, grain size is reduced to 180 ㎛ due to impurities at 318 ㎛. It can be seen that the red part is significantly reduced on the IPF image as well. In the ODF image, a peak is formed near the γ-fiber.

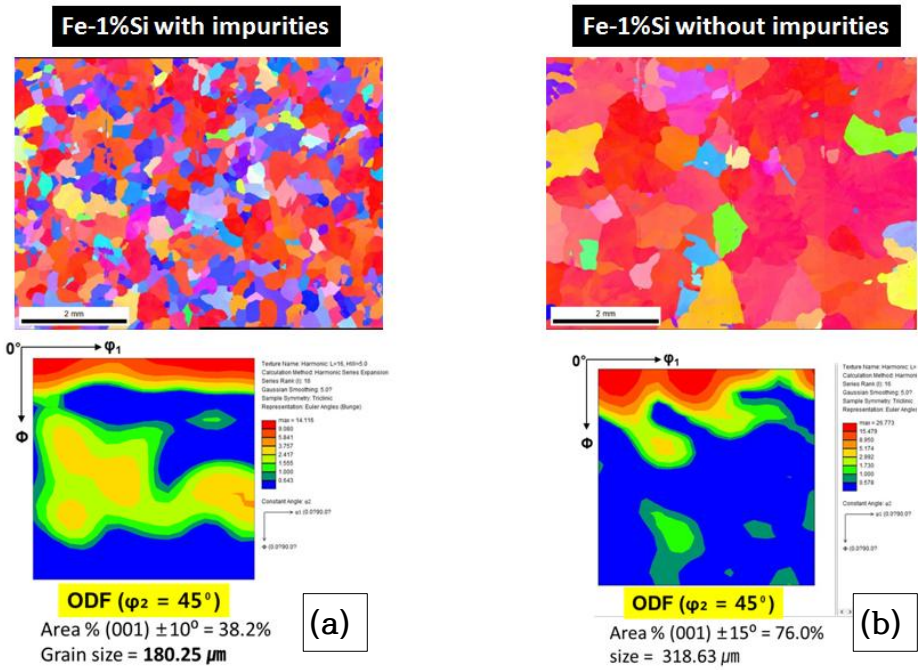

Fig 5.3 Texture and ODF (ϕ_2 =45^0) image of Fe-1%Si (a) with and (b) without impurities.

Finally, the effect of impurities can be considered as follows. Impurities reduce the grain size in the final specimen after the heat treatment process and interfere with the formation of the cube-on-face texture. This role of impurities is presumed to be as follows. Impurities firstly interfere with grain growth. This will result in grain formation in the γ phase being relatively small due to impurities. (Fig. 5.4) If the grain size of the γ phase is small, this plays a negative role in the formation of the cube-on-face texture.

This study assumes that the nucleation of the cube-on-face texture should occur on the surface. (chapter 2). This is because we think that 2D-stress must be applied during the nucleation process to form the seed of the cube-on-face. When nucleated at the surface, 2D-stress is most beneficial to receive, so if appropriate stress is applied, the grain nucleated on the surface will be mostly cube-on-face.

The nucleation barrier has a low energy at 4-grain corner and triple junction inside the bulk. [55] Therefore, if there are many such sites, some nucleation occurs inside the bulk. In the case of seeds generated in bulk, grains with different orientations other than cube-on-face are produced because they are not generated due to 2D stress. When these grow, there are grains with

orientations other than cube-on-face. [56,57] Therefore, in order to raise the area fraction of the cube-on-face texture, the nucleation should not occur inside the bulk. If the size of the grain increases, the nucleation sites inside the bulk such as the 4-grain corner will decrease. [58] Therefore, it is important to raise the grain size in the γ phase, and impurities are thought to be blocking it. As one piece of evidence for this, it can be considered that the grain size decreases with the composition containing impurities. This is because, as depicted in Fig. 5.4, the smaller the γ grain, the larger the nucleation sites and the smaller the grain size. [59]

Therefore, if impurities are inevitably included in the specimen during the mass production process, the process of increasing the γ grain size may reduce the nucleation site inside the bulk such as the 4-grain corner and the triple junction. In this way, the nucleation at the surface will dominate and the area fraction of the cube-on-face texture of the specimen will increase again.

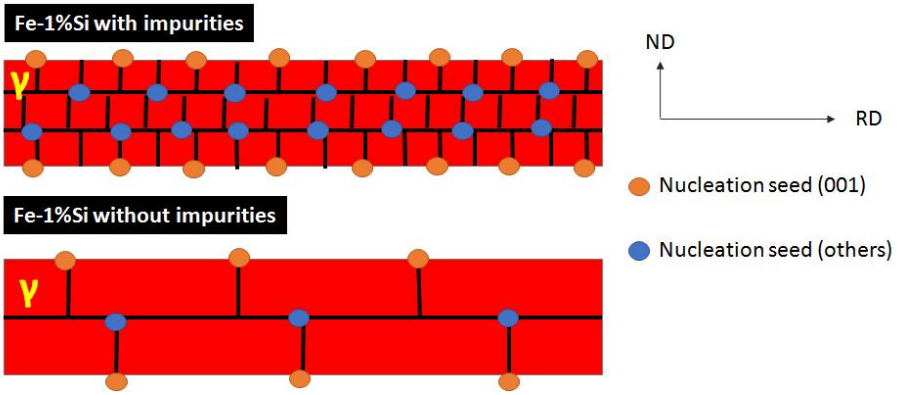

Fig 5.4 The schematic image of difference of the number of nucleation site at γ phase between with and without impurities.

Experiments such as Fig. 5.5 were designed and implemented to increase the grain size in the γ phase. The same specimens were kept in contact with the same alumina plate in the same atmosphere. Only the cooling rate was changed. Previous experiments had a cooling rate of 10 ℃ per minute from 1100 ℃ to 950 ℃, but in this experiment cooling was maintained at a cooling rate of 2.5 ℃ per minute. It is expected that the grain size of γ will be larger due to the longer holding time in the γ phase section. The upper part of Fig. 5.5 is the result of the previous experiment and the lower part is the experimental result of the longer cooling time.

Analysis of the specimen with EBSD showed that the area fraction of the cube-on-face texture increased significantly. By controlling the cooling rate, the existing 47.6% area fraction increased to 78.5%. Also, it can be seen that a denser cube-on-face texture is formed in the ODF image.

The conclusions of the preceding discussion have been confirmed through these experimental results. That is, the size of the γ grain determines the area fraction of the cube-on-face texture in the final texture. However, it was surprising that the size of the grain was reduced by 5%. If the γ grain grows heavily, the nucleation site will decrease and the absolute number

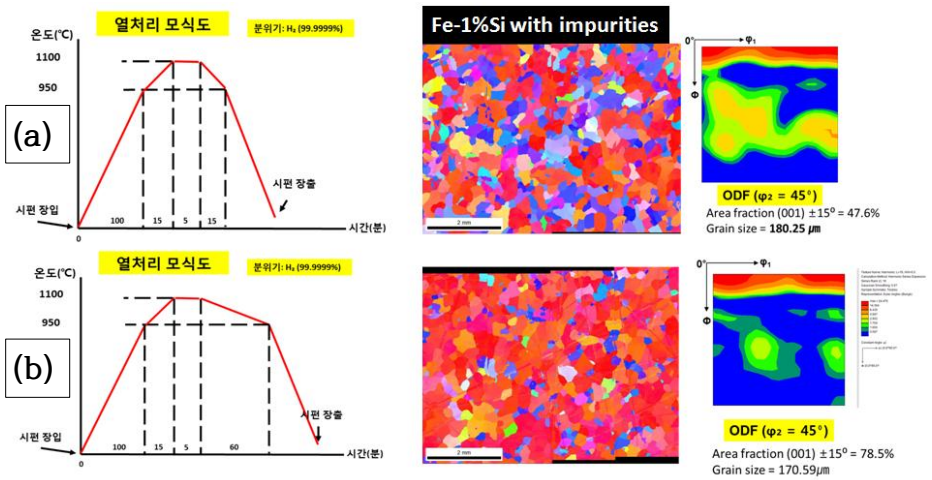

Fig 5.5 (a) Texture, ODF image and schematic image of heat treatment on Fe-1%Si with impurities (b) Texture, ODF image and schematic image of slow cooling heat treatment on Fe-1%Si with impurities.

of α grains will be insufficient. I thought that this would cause the grain to grow bigger, but I did not expect it to be.

5.3 Formation of cube-on-face texture with high Si content

As mentioned above, electrical steel has better performance when it contains more Si. Previously used specimens all contain 1% Si, while currently sold products contain 2 ~ 3% Si. Therefore, to form the cube-on-face texture, it is necessary to show that the cube-on-face texture is formed even in the high Si steel in order to help the actual process. Therefore, in this chapter, we will describe the ongoing research on the formation of cube-on-face texture in high Si steel.[60,61]

The high Si steel has problems. Si is an element that makes steel very brittle. Therefore, steel containing 3% or more of Si can not be cold rolled. In general, 3% Si steel is used as a limit. Another problem arises in the phase transform. The phase diagram of the Fe-Si system is shown in Fig. 5.6. Si is a typical α former and inhibits the formation of γ phase of Fe. When approximately 2% of Si enters, the γ phase disappears. The cube-on-face texture formation method used in this study uses a phase transform. [63] Therefore, if the Si content exceeds 2%, the present method can not be used. To solve these problems, many trial and error have been made. [64]

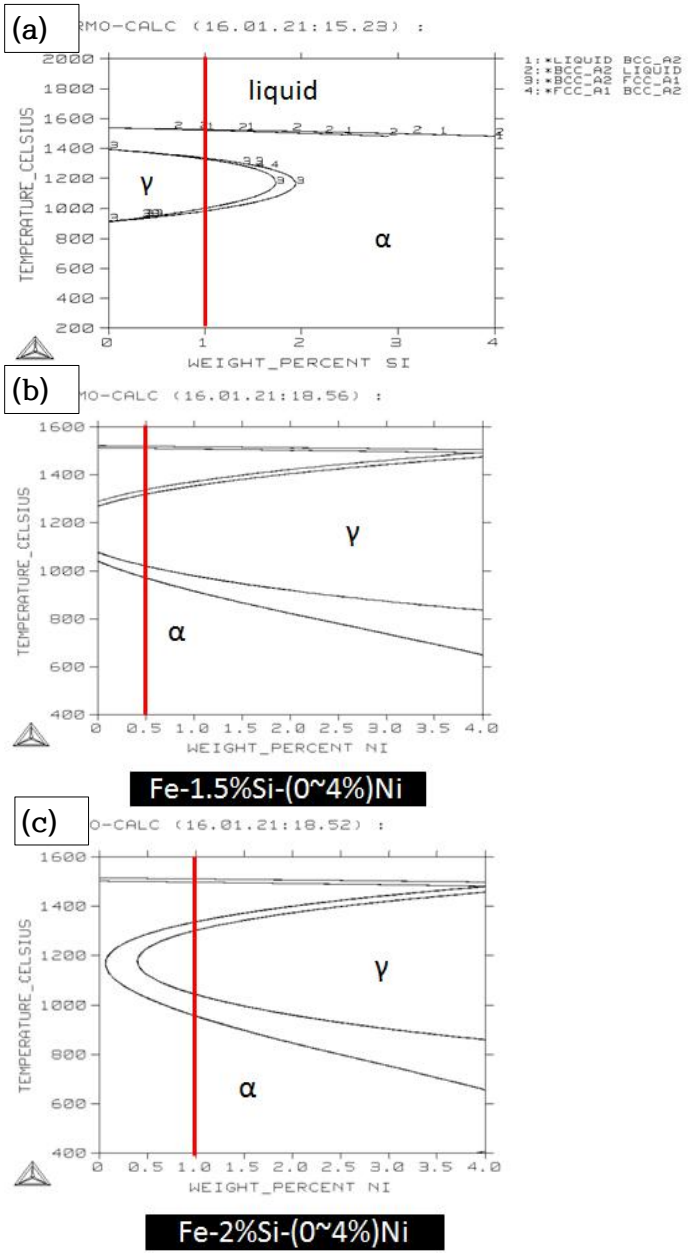

Fig 5.6 Phase diagram calculating from Thermo-calc about (a) Fe-Si, (b) Fe-1.5%Si-(0~4%)Ni and (c) Fe-2%Si-(0~4%)Ni

The γ formers were added to widen the γ phase region disappeared by Si. γ formers are representative of Mn, C, and Ni. [65,66] These are the elements that must be put in order to widen the γ region that has disappeared from the phase diagram by Si. Among them, Mn has a problem of volatilization at high temperature and is excluded. [67] C was excluded because grain growth did not occur constantly because precipitates were formed. [68] The most stable Ni was selected to serve as a γ former.

Fig. 5.6 shows the phase diagram of Fe-1.5% Si-Ni and Fe-2% Si-Ni, respectively. As the content of Ni increases, the area of γ becomes wider. This change in composition allowed us to widen the γ region that would be lost by Si.

(%)	C	Si	Mn	P	S	Al	Ti	N	Ni
Fe-1.5%Si-0.5%Ni	0.0022	1.5	0.055	0.005	0.0028	0.002	0.0016	0.0013	0.507
Fe-2%Si-1%Ni	0.0025	1.97	0.052	0.005	0.0034	0.003	0.0017	0.001	1.05

Fig 5.7 Chemical composition of 1.5%Si-0.5%Ni and 2%Si-1%Ni

Based on this understanding of phase diagram, the following composition was prepared. Fe-1.5% Si-0.5% Ni and Fe-2% Si-1% Ni were selected. There are the following reasons for this selection. In the case of the previously used Fe-1% Si steel, the phase transform is made between 1000℃ and 950℃. The amount of Ni was chosen so that all of the phase transforms occurred between 1050 and 950℃ by adjusting the amount of Ni to match this condition similarly.

After selecting the composition, samples of the above two compositions were prepared. A steel sheet with a thickness of 350 ㎛ was produced through hot rolling and cold rolling. The cube-on-face texture formation experiment was performed using this specimen. Although there are various methods of experiment, we decided to use U-type holder which has the best cube-on-face texture. The heat treatment was carried out by slowly cooling the specimen containing the impurities by reducing the cooling rate by 2.5 ℃ per minute. Figure 5.8 depicts this.

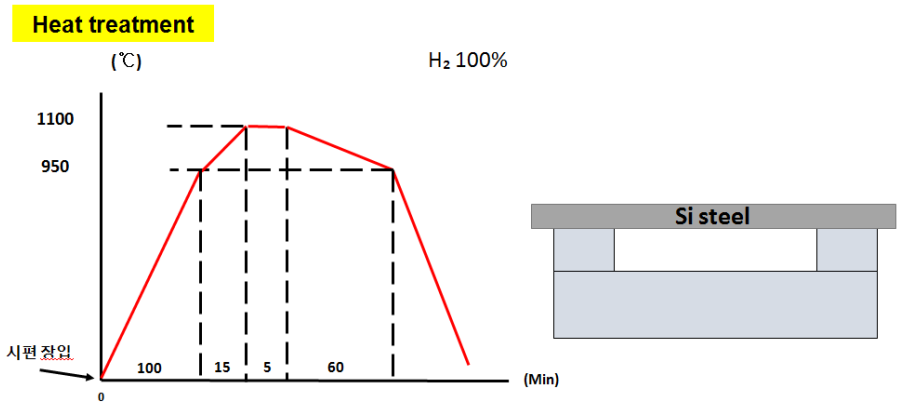

Fig 5.8 Schematic image of heat treatment on U-type holder experiment.

The 1.5%Si steel and the 2%Si steel were annealed and analyzed by EBSD. The results are summarized in Fig. 5.9. Figure 5.9 (a) shows the result of heat treatment of 1.5Si-0.5%Ni. Si was increased by 0.5% and cube-on-face texture was well formed even though Ni was added. On the IPF image, we can see that the red part representing the cube-on-face texture is spread widely. Also, the area fraction is 71.4%, showing high integration. It is a peculiar point that there are small grains with different orientations between the grains.

Fig. 5.9- (a) shows that cube-on-face texture is formed in 1.5% Si-0.5% Ni steel. On the other hand, the results of 5.9- (b) are slightly different. (b) is the result of EBSD analysis of 2% Si-1% Ni steel. (a), showing a typical recrystallized texture. The area fraction of the cube-on-face texture is 1.9%, which is very low. It is shown that Si and Ni are increased by 0.5% but show considerably different phase transform behavior. Furthermore, the grain size is 170 ㎛ for (a), but 99 ㎛ for (b) is relatively small. If you have undergone the same phase transform, you should have a similar grain size, but in this case it would be correct to say that you have seen different movements.

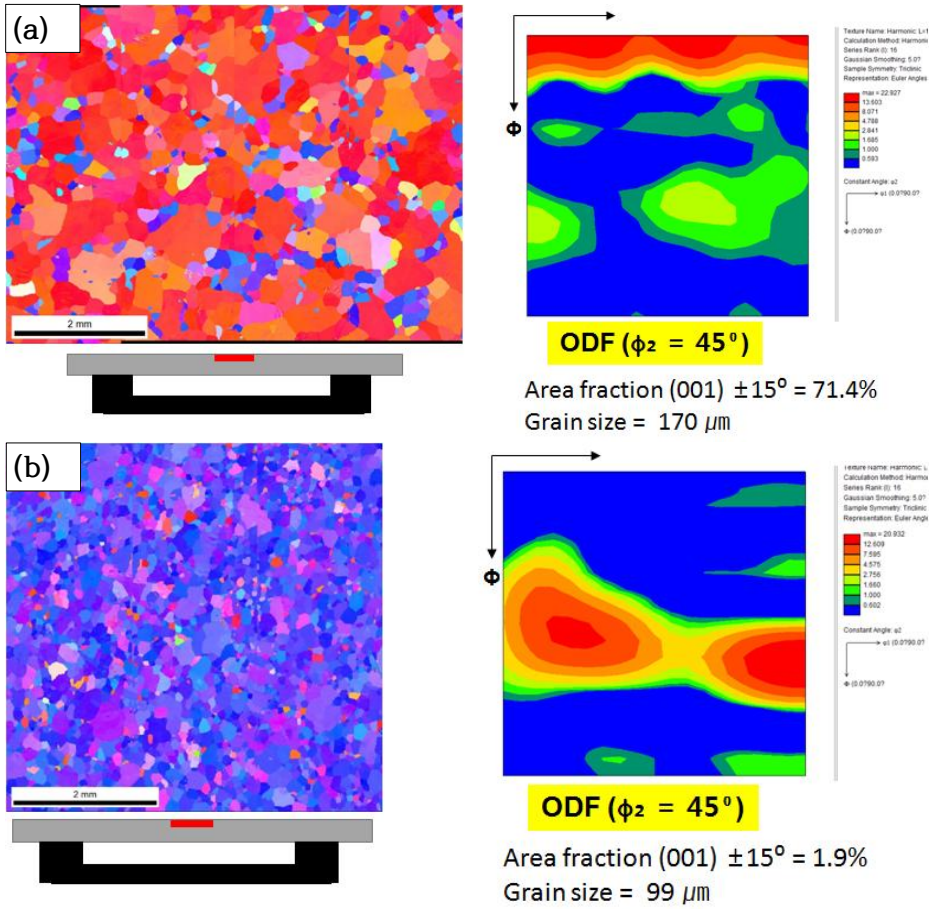

(c)	(001) Area fraction (±15°)	Grain size (㎛)
1%Si steel	88.1%	227
1%Si steel	90.9%	218
1%Si steel	88.1%	237
1.5%Si-0.5%Ni steel	71.4%	170
2%Si_1%Ni steel	1.9%	99

Fig 5.9 Texture and ODF image of (a) 1.5%Si-0.5%Ni and (b) 2%Si-1%Ni. (c) Area fraction and grain size of each composition form 1%Si to 2%Si-1%Ni

The conclusion to this point is that cube-on-face texture can be formed up to 1.5% Si steel by the above method. 2% Si steel has undergone dozens of experiments, but it has not been able to form a cube-on-face texture at present. While I was worried about these differences, I found interesting facts. Figure 5.9- (c) shows the result of summarizing the grain size of the previous experiments and the area fraction of the cube-on-face texture. It can be seen that the area fraction and grain size are proportional to each other. Although only a few representative cases are mentioned in the table, in practice, all the data that have been measured so far are analyzed and very proportionally very precisely fit. The grain size of the final α phase and the area fraction are related to each other. As a result, the inference about the γ grain size mentioned in Chapter 5.2 was recalled. As mentioned above, the larger the γ grain size, the better the surface nucleation and the better the cube-on-face texture is formed. Also, when the γ grain is large, the nucleation seed itself is reduced, and the number of grains in the α phase is reduced, thereby increasing the grain size. In other words, we could infer that the size of γ grain and the area fraction / α grain size are proportional to each other.

If so, we have come to the conclusion that the reason why the cube-on-face texture is not formed in 2%Si steel at present is

that the grain does not grow large in the γ phase for some reason. If this is the case, we thought that it would be easy to solve the problem by lengthening the heat treatment time in the γ section to increase the γ grain.

Based on these inferences, the following experiments were designed. Although the same experimental conditions as above were used, only the heat treatment time in the γ phase was controlled differently. 5 minutes, 2 hours, 12 hours, and 24 hours, respectively. After the same heat treatment, the specimens were analyzed by EBSD.

The result is shown in Fig. 5.11. As can be seen from the IPF image, it can be seen that the area fraction of the cube-on-face texture increases as the annealing time of the γ section becomes longer. (1.9% → 6.9% → 16.1% → 70.7%). Also, the grain size of the final α phase is also increased. (99 ㎛ → 114 ㎛ → 120 ㎛ → 223 ㎛) The method of explaining the increase of both the area fraction and the grain size can be explained only by the growth of the above-mentioned γ grain. Therefore, it can be said

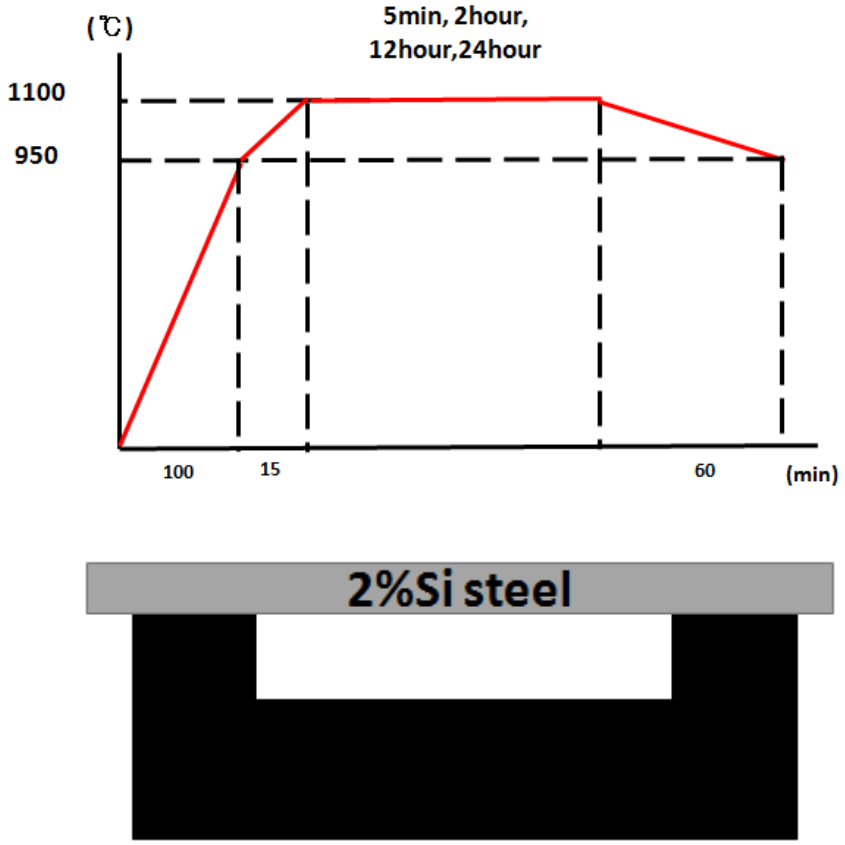

Fig 5.10 Schematic image of heat treatment 2%Si-1%Ni on U-type holder experiment at various γ phase keeping time

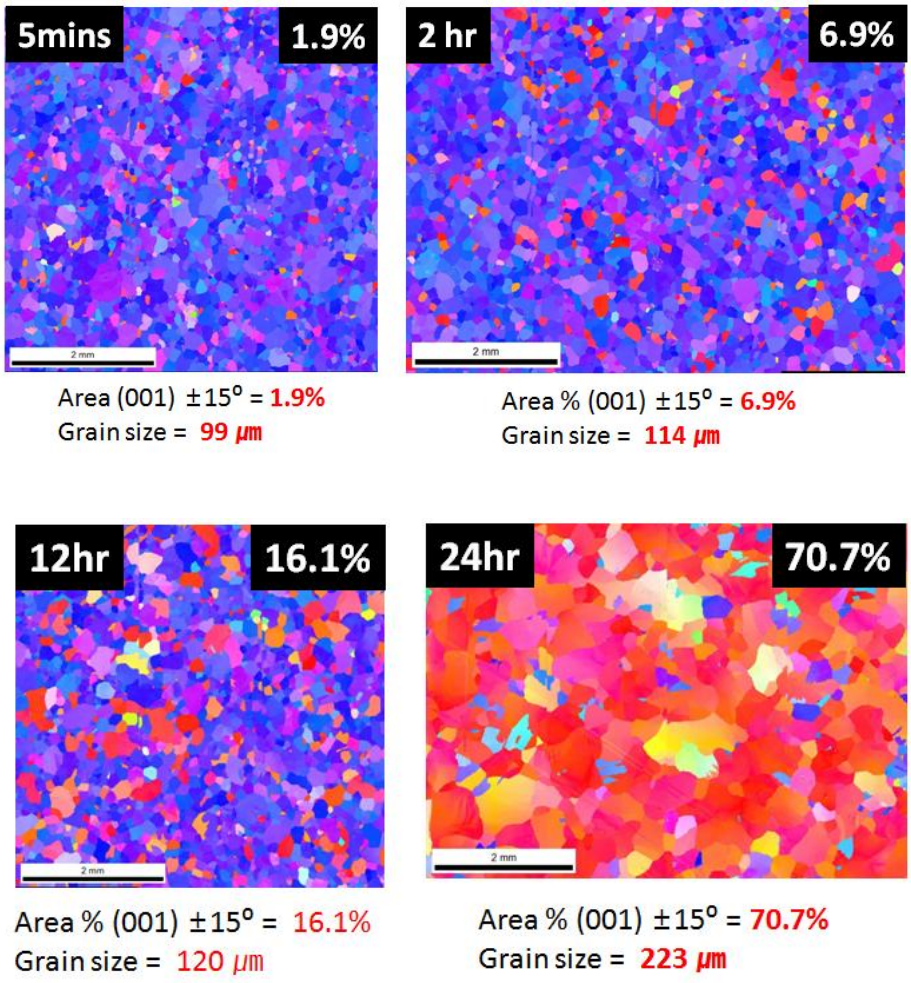

Fig 5.11 Texture, {001} area % and grain size of each γ phase heating time.

that the increase of the annealing time for growing the grain in the γ phase is effective.

No research team has shown a high area fraction of 70.7% without using vacuum in 2% Si steel. Therefore, based on these studies, we have wondered how to use it in actual production processes in the future. So far, the heat treatment time required to make a cube-on-face texture in 2% Si steel is about 30 hours. This long time was a problem, so I had a lot of worries about how to reduce the heat treatment time.

As a result, I got the following idea. If size is favorable for the formation of a cube-on-face texture with a large γ grain, it is doubtful that it can be raised even if the heat treatment is performed twice. At present, the heat treatment method is shifted from the α phase to the γ phase by raising the temperature. If the grain size of the initial α is increased, γ grain may not be increased. The following experiment was designed to confirm this.

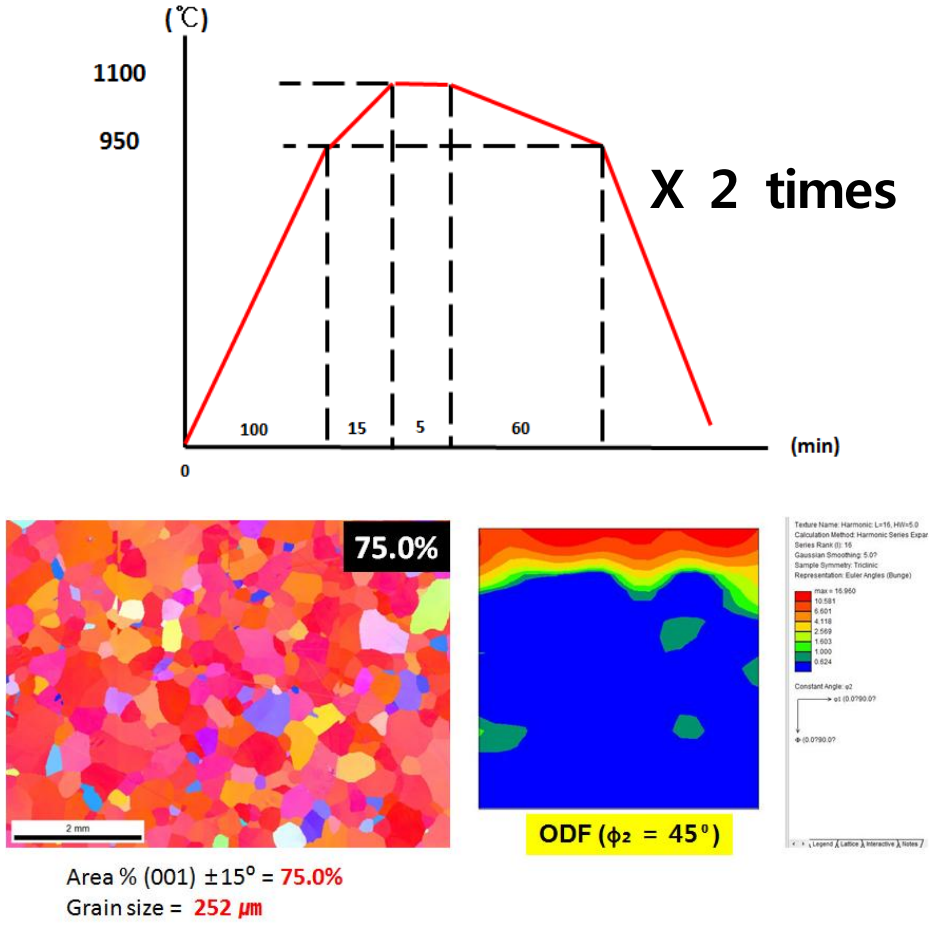

Fig 5.12 Schematic image of 2cycle heat treatment 2%Si-1%Ni. Texture, ODF image and area % of 2cycle specimen.

As shown in Fig. 5.12, the experiment was performed by repeating the heat treatment twice maintaining the γ phase section for 5 minutes. The results of the EBSD analysis of the specimen are also shown in Fig. 5.12.

As a result, cube-on-face texture was formed in 2% Si steel even in the 2-cycle heat treatment process. EBSD showed a structure with a high area fraction of 75.0% and a grain size of 252 ㎛. This experiment has shown that cube-on-face textures can be obtained from 2% Si steel even with relatively short heat treatments. We also concluded that cultivating the grain size in the γ phase would yield a cube-on-face texture.

6. Magnetic properties measurement

6.1 Introduction

Electrical steel is used to convert energy using the ability of Fe to be easier to magnetize than other materials, as mentioned in Chapter 1. There are many items that evaluate the magnetic properties of electrical steel. In the case of NO, there are two kinds of evaluation. The magnetic properties of electrical steel are evaluated by core loss and magnetic flux. The core loss is the amount of energy loss that occurs when rotating the hysteresis loop. This means the internal area of the hysteresis loop, the lower the efficiency, the better the motor. The core loss is measured under various conditions. In general, a relatively low frequency W15 / 50 and a high frequency W10 / 400 are measured and displayed. [69]

On the other hand, magnetic flux is a measure of how magnetization is achieved when a constant magnetic field is applied. The unit usually uses B50, which indicates the magnetization amount when a magnetic field of 5000 A / m is applied. It is an indicator of how much output can be produced when the same magnetic field is received. NO with low core loss

and high magnetic flux is said to be high quality electrical steel.

Cube-on-face texture is ideal for NO because it can lower core loss and increase magnetic flux through texture. Previously, only the composition and the microstructure were controlled by these two. However, since the texture can be controlled, researches on this are being actively carried out. We have succeeded in fabricating the cube-on-face texture, but since it has not yet been known how good the magnetic properties are, we made specimens and measured the magnetic properties. [70, 71]

6.2 Magnetic properties comparison with commercial steel

Experiments were conducted to investigate how the formation of the cube-on-face texture increases the magnetic performance in Si steel. In order to measure the magnetic properties, it is necessary to fabricate specimens of 50mm X 50mm size. This is because the minimum specimen size for measuring the magnetic properties is 50 mm x 50 mm. On the basis of our experience in Chapter 3, a 50mm x 50mm cube-on-face texture specimen was fabricated from 1% Si steel and 1.5% Si steel.

The cube-on-face specimens of 1% Si and 1.5% Si steel were prepared and the core loss and magnetic flux of the specimens

were measured. And the results are compared with the current mass production products. The commercial electrical steel are random textures. These comparisons will show how cube-on-face textures affect magnetic properties.

The measurement results are shown in Fig. 6.1. As mentioned above, electrical steel with low core loss (w15 / 50) and high magnetic flux (B50) is of high quality. The magnetic properties of commercial electrical steel are shown in Fig. 6.1 for comparison. Current commercial electrical steel contains more than 2% Si. In general, magnetic properties of electrical steel, which contains a lot of Si, are excellent. However, the 1% Si cube-on-face texture shows lower core loss and higher magnetic flux even with low Si content. 1.5% Si cube-on-face steel shows lower core loss and higher magnetic flux. The formation of the cube-on-face texture has led to improvements in magnetic properties. [72]

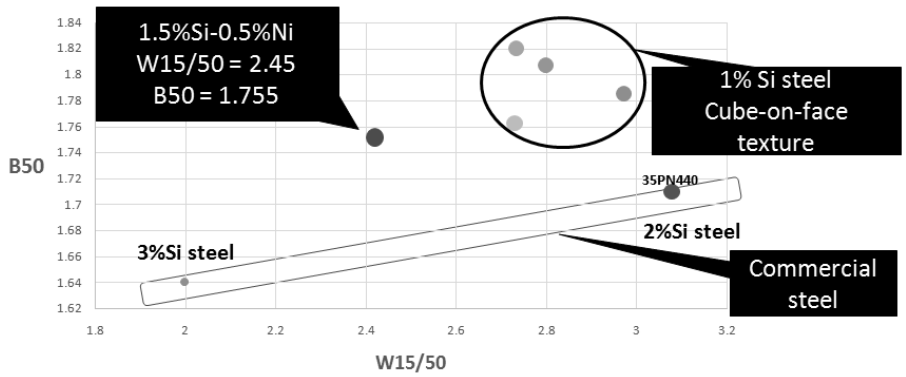

Fig 6.1 Graph about magnetic properties of cube-on-face texture specimen and commercial non-oriented electrical steel.

High-efficiency NO electrical steel increases the efficiency and power of the motor and increases the power generation efficiency of the power plant. Therefore, if a cube-on-face texture can be formed in high Si steel, energy efficiency can be greatly increased by using it. Therefore, the formation of cube-on-face texture in NO electrical steel is very valuable.

7. Conclusion

On non-oriented electrical steel, the ideal texture is cube-on-face texture. This is because the magnetic properties are good in the 2D direction. However, until now there is no know n method for forming cube-on-face textures on Si steel in a non-vacuum atmosphere. In particular, there has been no successful cube-on-face texture formation in steel containing more than 1% Si.

However, this study succeeded in forming cube-on-face texture of 1% Si steel in hydrogen atmosphere. An important factor in the formation of the cube-on-face texture is the small amount of stress applied during the phase transformation process. These stresses create conditions in which the cube-on-face texture is susceptible to nucleation when transforming from the α phase to the α phase.

There is a method of using the difference in thermal expansion coefficient as a method of applying such a fine stress. This method gives fine stress to the surface by shrinkage when cooling by contacting alumina plate or quartz plate with relatively low thermal expansion coefficient.

As a method of applying fine stress to the surface, there is a method of using self-weight. Using this method, we can fabricate Si steel with higher area fraction than previous plate method. Also, a cube-on-face texture can be formed using a U-type holder. Using this U-type holder, a high cube-on-face texture area fraction of 90.1% was obtained in 1% Si steel.

The higher the Si content of the electrical steel, the better the magnetic properties. However, it is very difficult to form a cube-on-face texture on steel containing more than 1% Si. In this study, we succeeded in forming a cube-on-face texture in 2% Si-1% Ni steel in a U-type holder by adjusting the heat treatment conditions so that the nucleation on the surface is well controlled. This is the first successful example in a hydrogen atmosphere other than a vacuum.

[1] P. Bate, B. Hutchinson, Effect of elastic interactions between displacive transformations on textures in steels, Acta Materialia, 48 (2000) 3183-3192.

[2] B.C. De Cooman, L. Chen, H.S. Kim, Y. Estrin, S.K. Kim, H. Voswinckel, State-of-the-science of high manganese TWIP steels for automotive applications, Microstructure and Texture in Steels, (2009) 165-183.

[3] D. Kohler, Promotion of cubic grain growth in 3% silicon iron by control of annealing atmosphere composition, Journal of Applied Physics, (1960) S408-S409.

[4] N. Sano, T. Tomida, S. Hinotani, A. Kuroda, H. Kotera, K. Fujiwara, Fine-grained and cube-textured Si-steel sheet hoop by oxide-separator-induced decarburization, in: INTERMAG Europe 2002 - IEEE International Magnetics Conference, 2002.

[5] T. Tomida, Magnetostrictive properties of cube-textured Si-steel sheets by oxide-separator-induced decarburization, in: INTERMAG Europe 2002 - IEEE International Magnetics Conference, 2002.

[6] M. Yabumoto, C. Kaido, T. Wakisaka, T. Kubota, N. Suzuki, Electrical steel sheet for traction motors of hybrid/electric vehicles, Nippon Steel Technical Report, (2003) 57-61.

[7] T. Tomida, A new process to develop (100) texture in silicon steel sheets, Journal of Materials Engineering and Performance, 5 (1996) 316-322.

[8] W.L. Elban, M.A. Hebbar, J.J. Kramer, Adsorption surface energy and crystal growth in lron-3 pct silicon, Metallurgical Transactions A, 6 (1975) 1929-1937.

[9] S.M. Shin, S. Birosca, S.K. Chang, B.C. De Cooman, Influence of

Normalizing Conditions on Electrical Steel Texture Development, in: Materials Science and Technology Conference and Exhibition, MS and T'07 - "Exploring Structure, Processing, and Applications Across Multiple Materials Systems", 2007, pp. 4008-4019.

[10] R. Saidur, A review on electrical motors energy use and energy savings, Renewable and Sustainable Energy Reviews, 14 (2010) 877-898.

[11] R.G. Aspden, J.A. Berger, H.E. Trout, Anisotropic and heterogeneous nucleation during the gamma to alpha transformation in iron, Acta Metallurgica, 16 (1968) 1027-1035.

[12] H. Wang, X. Huang, L. Xiang, S. Qiu, J. Wang, A new method to improve the density of favorable textures in non-oriented electrical steels, Metalurgia International, 18 (2013) 9-14.

[13] J.L. Routbort, C.N. Reid, E.S. Fisher, D.J. Dever, High-temperature elastic constants and the phase stability of silicon-iron, Acta Metallurgica, 19 (1971) 1307-1316.

[14] H. Shimanaka, T. Irie, K. Matsumura, H. Nakamura, A new non-oriented Si-steel with texture of {100} 〈ovw〉, Journal of Magnetism and Magnetic Materials, 19 (1980) 63-64.

[15] C.F. Chang, R.L. Bye, V. Laxmanan, S.K. Das, Texture and Magnetic Properties of Rapidly Quenched Fe-6.5wt%Si Ribbon, IEEE Transactions on Magnetics, 20 (1984) 553-558.

[16] O. Hashimoto, S. Satoh, T. Tanaka, FORMATION OF alpha yields gamma yields alpha TRANSFORMATION TEXTURE IN SHEET STEEL, Transactions of the Iron and Steel Institute of Japan, 23 (1983) 1028-1037.

[17] S.M. Park, Y.M. Koo, B.Y. Shim, D.N. Lee, Effects of process variables in decarburization annealing of Fe-3%Si-0.3%C steel sheet on

textures and magnetic properties, Metals and Materials International, 23 (2017) 220-232.

[18] L. Xie, P. Yang, N. Zhang, W. Mao, Texture Optimization for Intermediate Si-Containing Non-oriented Electrical Steel, Journal of Materials Engineering and Performance, 23 (2014) 3849-3858.

[19] H.K.D.H. Bhadeshia, Diffusional formation of ferrite in iron and its alloys, Progress in Materials Science, 29 (1985) 321-386.

[20] T.B. Massalski, Massive transformations revisited, Metallurgical and Materials Transactions A: Physical Metallurgy and Materials Science, 33 (2002) 2277-2283.

[21] L. Zhang, P. Yang, W. Mao, Opposite Relationship between Orientation Selection and Texture Memory in the Deformed Electrical Steel Sheets during α→γ→α Transformation, Journal of Materials Science and Technology, 33 (2017) 1522-1530.

[22] L. Xie, P. Yang, Review of the preparation methods of {100} texture in non-oriented electrical steels, Cailiao Rechuli Xuebao/Transactions of Materials and Heat Treatment, 34 (2013) 9-17.

[23] R.G. Aspden, J.A. Berger, H.E. Trout, New texture in iron and iron base alloys, Journal of Applied Physics, 37 (1966) 1195-1196.

[24] B. De Boer, J. Wieting, Formation of a near {001}〈110〉 recrystallization texture in electrical steels, Scripta Materialia, 37 (1997) 753-760.

[25] M. Takashima, M. Komatsubara, N. Morito, {001}〈210〉 Texture development by two-stage cold rolling method in non-oriented electrical steel, ISIJ International, 37 (1997) 1263-1268.

[26] T. Tomida, S. Uenoya, Cube oriented 3%Si-1%Mn soft magnetic steel sheets with fine grain structure, IEEE Transactions on Magnetics,

37 (2001) 2318-2320.

[27] J. Harase, R. Shimizu, N. Takahashi, Coincidence grain boundary and (100) [001] secondary recrystallization in Fe-3% Si, Acta Metallurgica Et Materialia, 38 (1990) 1849-1856.

[28] X. Huang, L. Xiang, S. Qiu, Z. Song, Effect of copper on surface texture of non-oriented electrical steel plate, Jinshu Rechuli/Heat Treatment of Metals, 38 (2013) 31-35.

[29] A. Bodin, L. Woning, J. Sietsma, S. Van Der Zwaag, In-situ high-temperature X-ray diffraction on the γ→α transformation in low-carbon steels, ISIJ International, 42 (2002) 94-99.

[30] D.J. Dever, Temperature dependence of the elastic constants in α-iron single crystals: Relationship to spin order and diffusion anomalies, Journal of Applied Physics, 43 (1972) 3293-3301.

[31] J. Berger, F. Thomas, J. Berthon, A. Revcolevschi, Elastic properties of Fe1-xO near the antiferromagnetic phase transition, Solid State Communications, 48 (1983) 231-233.

[32] N. Zhang, P. Yang, W. Mao, Influence of columnar grains on the cold Rolling texture evolution in Fe-3%Si electrical steel, Jinshu Xuebao/Acta Metallurgica Sinica, 48 (2012) 782-788.

[33] N. Zhang, P. Yang, W. Mao, Influence of columnar grains on the recrystallization texture evolution in Fe-3%Si electrical steel, Jinshu Xuebao/Acta Metallurgica Sinica, 48 (2012) 307-314.

[34] D. Xia, P. Yang, L. Xie, W. Mao, Influence of heating rate on the decarburized annealing microstructure and texture in low-carbon non-oriented electrical steel, Jinshu Xuebao/Acta Metallurgica Sinica, 50 (2014) 1437-1445.

[35] J.K. Sung, D.N. Lee, D.H. Wang, Y.M. Koo, Efficient generation of

cube-on-face crystallographic texture in iron and its alloys, ISIJ International, 51 (2011) 284-290.

[36] J. Wang, P. Yang, L. Zhang, W. Mao, Formation of a sharp {100} 〈 011 〉 texture in Fe - 3 %Si - 1.7 %Mn - 0.05 %C silicon steel sheets, Journal of Materials Science, 51 (2016) 10116-10126.

[37] L. Zhang, P. Yang, J. Wang, W. Mao, Transformation of {100} texture induced by surface effect in ultra-low carbon electrical steel, Journal of Materials Science, 51 (2016) 8087-8097.

[38] J. Wang, P. Yang, W. Mao, Retention and evolution of texture in an electrical steel under vacuum annealing, Journal of Materials Science, 52 (2017) 5462-5473.

[39] L. Zhang, P. Yang, W. Mao, Phenomena of Σ3 and orientation gradients in an electrical steel applied α→γ→α transformation, Jinshu Xuebao/Acta Metallurgica Sinica, 53 (2017) 19-30.

[40] T. Tomida, Decarburization of silicon steel sheets by silicon dioxide and development of {100} 〈012〉 texture, Nippon Kinzoku Gakkaishi/Journal of the Japan Institute of Metals, 66 (2002) 824-831.

[41] T. Tomida, S. Uenoya, N. Sano, Fine-grained doubly-oriented electrical steel sheets and mechanism of cube texture development, Nippon Kinzoku Gakkaishi/Journal of the Japan Institute of Metals, 66 (2002) 950-957.

[42] L. Cheng, N. Zhang, P. Yang, W.M. Mao, Retaining {1 0 0} texture from initial columnar grains in electrical steels, Scripta Materialia, 67 (2012) 899-902.

[43] W.S. Ko, J.Y. Park, J.Y. Byun, J.K. Lee, N.J. Kim, B.J. Lee, Manipulation of surface energy anisotropy in iron using surface segregation of phosphorus: An atomistic simulation, Scripta Materialia,

68 (2013) 329-332.
[44] F. Katsuki, T. Tomida, H. Nakatani, M. Katoh, A. Takata, Development of a thermoelectric power generation system using reciprocating flow combustion in a porous FeSi2 element, Review of Scientific Instruments, 72 (2001) 3996-3999.
[45] T. Tomida, (100)-textured 3% silicon steel sheets by manganese removal and decarburization, Journal of Applied Physics, 79 (1996) 5443-5445.
[46] Y. He, E. Hilinski, M. Attard, D. Bibby, R. Santos, R. Zavadil, Influence of the angle between cold rolling direction and hot rolling direction on the texture evolution of non-oriented electrical steels, in: IOP Conference Series: Materials Science and Engineering, 2015.
[47] Y.B. Xu, Y.X. Zhang, Y. Wang, C.G. Li, G.M. Cao, Z.Y. Liu, G.D. Wang, Evolution of cube texture in strip-cast non-oriented silicon steels, Scripta Materialia, 87 (2014) 17-20.
[48] N. Zhang, P. Yang, W. Mao, Formation of cube texture affected by neighboring grains in a transverse-directionally aligned columnar-grained electrical steel, Materials Letters, 93 (2013) 363-365.
[49] J. Kyung Sung, Y. Mo Koo, Magnetic properties of Fe and Fe-Si alloys with {100}0vw texture, Journal of Applied Physics, 113 (2013).
[50] C. Kaido, T. Wakisaka, Effect of material parameters on iron losses in non-oriented electrical steel sheets, T. IEE Japan, 117 A (1997) 685-690.
[51] N.R. Overman, X. Jiang, R.K. Kukkadapu, T. Clark, T.J. Roosendaal, G. Coffey, J.E. Shield, S.N. Mathaudhu, Physical and electrical properties of melt-spun Fe-Si (3 - 8 wt.%) soft magnetic ribbons, Materials Characterization, 136 (2018) 212-220.

[52] A.J. Moses, Electrical steels. Past, present and future developments, IEE Proceedings A: Physical Science. Measurement and Instrumentation. Management and Education. Reviews, 137 (1990) 233-245.

[53] K. Abiko, K. Sadamori, The role of carbon on the α → γ transformation behavior in high-purity iron, Physica Status Solidi (A) Applied Research, 167 (1998) 275-287.

[54] M. Nakano, T. Okamoto, H. Fukunaga, Y. Yamashiro, K. Ishiyama, K.I. Arai, Ultra-low iron loss in new non-oriented silicon steel sheets, Journal of Magnetism and Magnetic Materials, 196 (1999) 341-343.

[55] S.M. Shin, S. Birosca, S.K. Chang, B.C. De Cooman, Texture evolution in grain-oriented electrical steel during hot band annealing and cold rolling, Journal of Microscopy, 230 (2008) 414-423.

[56] H. Kimizuka, H. Kaburaki, Molecular dynamics study of the high-temperature elasticity of SiO 2 polymorphs: Structural phase transition and elastic anomaly, Physica Status Solidi (B) Basic Research, 242 (2005) 607-620.

[57] R.M.S.B. Horta, W.T. Roberts, D.V. Wilson, Texture representation by inverse pole figures, Trans. Metall. Soc. AIME, 245 (1969).

[58] F.J.G. Landgraf, T. Yonamine, R. Takanohashi, F.Q. Silva, J.P.V. Tosetti, F.B. Neto, E. Albertin, V.N.G. Mazzarella, I.G.S. Falleiros, M. Emura, Magnetic properties of silicon steel with as-cast columnar structure, Journal of Magnetism and Magnetic Materials, 254-255 (2003) 364-366.

[59] T. Tomida, N. Sano, K. Ueda, K. Fujiwara, N. Takahashi, Cube-textured Si-steel sheets by oxide-separator-induced decarburization and growth mechanism of cube grains, Journal of Magnetism and Magnetic Materials, 254-255 (2003) 315-317.

[60] F. Kovác, M. Dzubinský, Y. Sidor, Columnar grain growth in non-oriented electrical steels, Journal of Magnetism and Magnetic Materials, 269 (2004) 333-340.
[61] L. Xie, P. Yang, N. Zhang, C. Zong, D. Xia, W. Mao, Formation of {1 0 0} textured columnar grain structure in a non-oriented electrical steel by phase transformation, Journal of Magnetism and Magnetic Materials, 356 (2014) 1-4.
[62] L. Xie, P. Yang, D. Xia, W. Mao, Microstructure and texture evolution in a non-oriented electrical steel during γ→α transformation under various atmosphere conditions, Journal of Magnetism and Magnetic Materials, 374 (2015) 655-662.
[63] M. Džubinský, Y. Sidor, F. Kováč, Kinetics of columnar abnormal grain growth in low-Si non-oriented electrical steel, Materials Science and Engineering A, 385 (2004) 449-454.
[64] H. Pan, Z. Zhang, Y. Mo, J. Xie, Strong 〈001〉 recrystallization texture component in 6.5 wt% Si electrical steel thin sheets by secondary cold rolling and annealing, Journal of Magnetism and Magnetic Materials, 419 (2016) 500-511.
[65] D.N. Lee, Elastic properties of thin films of cubic system, Thin Solid Films, 434 (2003) 183-189.
[66] R. Liang, P. Yang, W. Mao, Retaining {1 0 0} texture from initial columnar grains in 6.5 wt% Si electrical steels, Journal of Magnetism and Magnetic Materials, 441 (2017) 511-516.
[67] N. Yoshinaga, L. Kestens, B.C. De Cooman, α→γ→α transformation texture formation at cold-rolled ultra low carbon steel surfaces, in: Materials Science Forum, 2005, pp. 1267-1272.
[68] P. Błoński, A. Kiejna, Structural, electronic, and magnetic properties

of bcc iron surfaces, Surface Science, 601 (2007) 123-133.
[69] J.K. Sung, S.M. Park, B.Y. Shim, Y.M. Koo, Effect of Mn on <100> texture evolution in Fe-Si-Mn alloys, in: Materials Science Forum, 2012, pp. 730-733.
[70] A. Salinas-Rodríguez, E. Gutiérrez-Castañeda, Processing and microstructure of grain non-oriented electrical steel strips with improved magnetic properties, in: Materials Science Forum, 2012, pp. 2800-2805.
[71] J.K. Sung, D.N. Lee, Evolution of crystallographic texture in pure iron and commercial steels by γ to α transformation, in: Materials Science Forum, 2012, pp. 2657-2662.
[72] L. Kestens, S. Jacobs, Texture control during the manufacturing of nonoriented electrical steels, Texture, Stress, and Microstructure, 2008 (2008).

요약 (국문 초록)

철의 자기적 특성을 이용하는 전기 강판은 방향성 전기강판과 무방향성 전기강판으로 분류한다. 무방향성 전기 강판의 경우 일반적으로 회전하는 모터나 발전기 내부에 주로 사용된다. 최근 산업계에서 전기차와 발전기에 대한 효율에 관심이 많아졌다. 이에 고효율 무방향성 전기 강판에 대한 관심이 매우 높아지고 있다. 일반적으로 철강의 특성은 조성, 미세조직, 집합조직을 통해 제어가 된다. 무방향성 전기 강판의 경우 이 세 가지 변수를 제어하여 높은 자기적 특성을 나타내려 하고 있다. 조성과 미세조직의 이미 많은 연구와 최적화가 이루어진 상황이다. 하지만 집합조직을 제어하는 것에는 아직 많은 연구의 진전이 이루어지지지 않았다.

cube-on-face 집합조직은 무방향성 전기 강판에서 이상적인 집합조직으로 알려져 있다. 하지만, cube-on-face 집합조직을 이용하는 무방향성 전기 강판은 아직 생산되지 않고 있다. 본 연구에서는 무방향성 전기 강판의 형성하는데 어떠한 조건이 필요한지를 밝혀 내려한다. 또한 고 Si steel에서 cube-on-face texture를 형성시키는데 필요한 조건이 무엇인지 밝히고자 한다.

감마 -> 알파 상변태에서 미세한 응력을 가해주면 cube-on-face 집합조직이 형성된다. 이러한 결과를 바탕으로 본 연구팀은 cube-on-face 집합조직을 가지는 대면적 시편을 제작하는데 성공하

였다. 더 나아가 자중을 이용하여 다양한 방법으로 시편에 응력을 가해주는 방법을 고안하였고, 이를 이용하여 cube-on-face 집합조직을 형성시키는데 성공하였다. 감마 -> 알파 상변태 과정에서 알파 핵생성 장소를 제어하여 cube-on-face 집합조직의 핵생성이 더 쉽게 일어나게 하였고, 이를 통하여 1%~2%Si 강에서 cube-on-face 집합조직을 형성시키는 것에 성공하였다.

주요어 (主要語) : 무방향성 전기강판; 자기적 특성; 집합조직 제어; 상변태; Cube-on-face 집합조직,

학번 : 2014-31049